

UNCLASSIFIED

AD NUMBER

AD855874

LIMITATION CHANGES

TO:

Approved for public release; distribution is unlimited. Document partially illegible.

FROM:

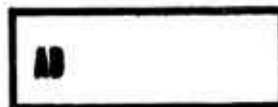
Distribution authorized to U.S. Gov't. agencies and their contractors; Critical Technology; JUN 1969. Other requests shall be referred to Army Aviation Materiel Labs., Fort Eustis, VA. Document partially illegible. This document contains export-controlled technical data.

AUTHORITY

USAAMRDL ltr dtd 18 Jun 1971

THIS PAGE IS UNCLASSIFIED

AD855874



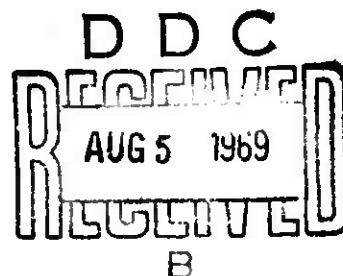
**USAAVLABS TECHNICAL REPORT 69-17**

**RELIABILITY EVALUATION OF A MECHANICAL  
STABILITY AUGMENTATION SYSTEM  
FOR HELICOPTERS**

By

Mario M. George  
Eugene Kisielowski  
Edmund M. Fraundorf

June 1969



**U. S. ARMY AVIATION MATERIEL LABORATORIES  
FORT EUSTIS, VIRGINIA**

**CONTRACT DAAJ02-67-C-0029  
DYNASCIENCES CORPORATION  
BLUE BELL, PENNSYLVANIA**



### Disclaimers

The findings in this report are not to be construed as an official Department of the Army position unless so designated by other authorized documents.

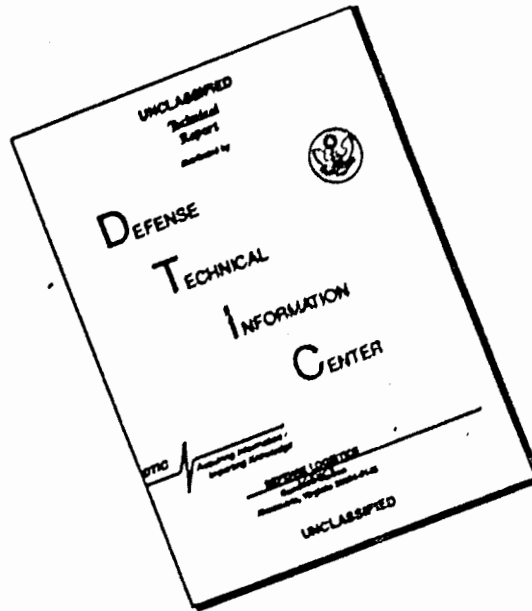
When government drawings, specifications, or other data are used for any purpose other than in connection with a definitely related Government procurement operation, the United States Government thereby incurs no responsibility nor any obligation whatsoever; and the fact that the Government may have formulated, furnished, or in any way supplied the said drawings, specifications, or other data is not to be regarded by implication or otherwise as in any manner licensing the holder or any other person or corporation, or conveying any rights or permission, to manufacture, use, or sell any patented invention that may in any way be related thereto.

### Disposition Instructions

Destroy this report when no longer needed. Do not return it to the originator.

DISPOSITION FOR	
POSTI	WHITE SECTION <input type="checkbox"/>
IPC	BUFF SECTION <input checked="" type="checkbox"/>
ANNOUNCED	<input type="checkbox"/>
JUSTIFICATION	<input type="checkbox"/>
BY: <i>per [signature]</i>	
DISTRIBUTION/AVAILABILITY CODES	
REQ.	AVAIL. and/or SPECIAL
<i>91</i>	

# DISCLAIMER NOTICE



THIS DOCUMENT IS BEST QUALITY AVAILABLE. THE COPY FURNISHED TO DTIC CONTAINED A SIGNIFICANT NUMBER OF PAGES WHICH DO NOT REPRODUCE LEGIBLY.



DEPARTMENT OF THE ARMY  
U. S. ARMY AVIATION MATERIEL LABORATORIES  
FORT EUSTIS, VIRGINIA 23604

This report has been reviewed by the U. S. Army Aviation Materiel Laboratories and is considered to be technically sound. The report is published for the exchange of information and the stimulation of ideas.

Task 1F162204A13905  
Contract DAAJ02-67-C-0029  
USAAVLABS Technical Report 69-17  
June 1969

RELIABILITY EVALUATION OF A MECHANICAL  
STABILITY AUGMENTATION SYSTEM  
FOR HELICOPTERS

Dynasciences Report DCR-284

By

M. George  
E. Kisielowski  
E. Fraundorf

Prepared by

Dynasciences Corporation  
Blue Bell, Pennsylvania  
STATEMENT #2 UNCLASSIFIED

This document is subject to special export controls and each  
transmittal to foreign governments or foreign nationals may be  
made only with prior approval of \_\_\_\_\_

U. S. ARMY AVIATION MATERIEL LABORATORIES  
FORT EUSTIS, VIRGINIA



## SUMMARY

This report presents the results of a reliability evaluation of a flightworthy, compact, lightweight three-axis mechanical stability augmentation system (MSAS) for helicopters. The MSAS consists of the DYNAGYRO, a two-axis coulomb damped gyroscope, and the Heading Assist Gyro, a single-axis spring-damped rate gyroscope. As part of this program, a prototype flightworthy model of the MSAS was designed, fabricated and extensively tested to evaluate the reliability and maintainability of the system. The results of these tests have demonstrated that the MSAS has excellent stability augmentation characteristics, is mechanically reliable, and is easy to maintain.

### FOREWORD

The work reported herein is part of a continuing effort by Dynasciences Corporation to provide V/STOL aircraft with a stabilization system that is reliable, lightweight, compact, inexpensive, and easy to maintain. This work was performed for the U. S. Army Aviation Materiel Laboratories (USAAVLABS), Fort Eustis, Virginia, under Contract DAAJ02-67-C-0029, Task 1F162204A13905, during the period from March 1967 to December 1968.

The program was under the cognizance of Mr. George Fosdick, U. S. Army project engineer, whose many contributions toward successful accomplishment of this work are gratefully acknowledged.

The following Dynasciences Corporation personnel contributed to this program:

Mr. M. George, Program Manager  
Mr. E. Fraundorf, Test Engineer  
Mr. R. R. Kenworthy, Senior Design Engineer  
Mr. E. Kisielowski, Deputy Director, Aero Research  
Mr. H. G. Somerson, Director of Engineering



## TABLE OF CONTENTS

	<u>Page</u>
SUMMARY . . . . .	111
FOREWORD . . . . .	v
LIST OF ILLUSTRATIONS . . . . .	viii
LIST OF TABLES . . . . .	xi
LIST OF SYMBOLS . . . . .	xii
I. INTRODUCTION . . . . .	1
II. SYSTEM DESCRIPTION . . . . .	3
III. ANALOG COMPUTER SIMULATION OF THE HUGHES 269-A HELICOPTER EQUIPPED WITH THE MSAS . . . . .	9
IV. RELIABILITY EVALUATION OF THE MSAS . . . . .	43
V. CONCLUSIONS AND RECOMMENDATIONS . . . . .	68
VI. REFERENCES . . . . .	69
APPENDIX - CHRONOLOGICAL HISTORY, MSAS TEST PROGRAM . . . . .	70
DISTRIBUTION . . . . .	81

## LIST OF ILLUSTRATIONS

<u>Figure</u>		<u>Page</u>
1	Reliability Evaluation Test Setup of the MSAS . . . . .	4
2	Exploded View of MSAS Components . . . . .	5
3	Schematic Representation of MSAS Mixing in a Helicopter Control System . . . . .	6
4	Analog Computer Schematic . . . . .	13
5	Response of the 269-A Helicopter (Half-Tail) to a Pulse Control Input (Hover) . . . . .	19
6	Response of the 269-A Helicopter (Half-Tail) to a Pulse Control Input (35 Knots) . . . . .	23
7	Response of the 269-A Helicopter (Half-Tail) to a Pulse Control Input (70 Knots). . . . .	27
8	Effect of Dynagyro Stabilizer Parameters on the Longitudinal Characteristics of the 269-A Helicopter (Hover) . . . . .	31
9	Effect of Dynagyro Stabilizer Parameters on the Longitudinal Characteristics of the 269-A Helicopter (35 Knots). . . . .	32
10	Effect of Dynagyro Stabilizer Parameter on the Longitudinal Characteristics of the 269-A Helicopter (70 Knots). . . . .	33
11	Effect of Dynagyro Stabilizer Parameters on the Lateral Dynamic Characteristics of the 269-A Helicopter (Hover) . . . . .	34
12	Effect of Dynagyro Stabilizer Parameters on the Lateral Dynamic Characteristics of the 269-A Helicopter (35 Knots). . . . .	35

<u>Figure</u>		<u>Page</u>
13	Effect of Dynagyro Stabilizer Parameters on the Lateral Dynamic Characteristics of the 269-A Helicopter (70 Knots) . . .	36
14	Effect of the Heading Assist Gyro Stabilizer Parameters on the Directional Characteristics of the 269-A Helicopter (Hover) . . . . .	38
15	Effect of the Heading Assist Gyro Stabilizer Parameters on the Directional Characteristics of the 269-A Helicopter (35 Knots) . . . . .	39
16	Effect of the Heading Assist Gyro Stabilizer Parameters on the Directional Characteristics of the 269-A Helicopter (70 Knots) . . . . .	40
17	Time Constant for Aircraft Longitudinal Velocity Response Versus Rotor Advance Ratio for Various Pilot/Dynagyro Authority Ratios, $R = 0.0075$ . . . . .	41
18	Time Constant for Aircraft Lateral Velocity Response Versus Rotor Advance Ratio for Various Pilot/Dynagyro Authority Ratios, $R = 0.0075$ . . . . .	42
19	Test Apparatus of MSAS During Reliability Evaluation . . . . .	44
20	Block Diagram of the MSAS Hydraulic System	45
21	Block Diagram of the MSAS Test Circuitry	48
22	Time History Response of the Dynagyro to a Step Input . . . . .	53
23	Time History Response of the Dynagyro to Sinusoidal Input . . . . .	54

<u>Figure</u>		<u>Page</u>
24	Time History Response of the Heading Assist Gyro to a Step Input . . . .	55
25	Time History Response of the Heading Assist Gyro to a Sinusoidal Input . . . .	56
26	Dynagyro Damping Rate History Versus Cumulative Test Hours . . . . .	58
27	Dynagyro Precessional Coupling Versus Cumulative Test Hours . . . . .	59
28	Heading Assist Gyro Damping Ratio Versus Cumulative Test Hours . . . . .	61
29	Heading Assist Gyro Phase Angle Versus Cumulative Test Hours . . . . .	63

## LIST OF TABLES

	<u>Page</u>
I MSAS Specifications . . . . .	8
II Total Stability Derivatives . . . . .	15
III Reliability Evaluation Test Cycle of MSAS	47
IV MSAS Instrumentation Summary . . . . .	49
V Test Hour Summary of MSAS . . . . .	52
VI Modified Damper Assembly Wear Summary . . . . .	79

### LIST OF SYMBOLS

$A_{1s}$	lateral cyclic control due to stabilizer input, rad
$A_{1c}$	lateral cyclic control due to pilot input, rad
$B_{1s}$	longitudinal cyclic control due to stabilizer input, rad
$B_{1c}$	longitudinal cyclic control due to pilot input, rad
$C_D$	specific damping coefficient, in-lb-sec/rad
$I_s$	mass moment of inertia of gyro wheel, slug-ft <sup>2</sup>
$J_1$	pilot's longitudinal cyclic control authority ratio, 1 - $k_1$
$J_2$	pilot's lateral cyclic control authority ratio, 1 - $k_2$
$J_3$	pilot's directional cyclic control authority ratio, 1 - $k_3$
$k_s$	spring constant, in-lb/rad
$k_1$	gyro to pilot longitudinal control authority ratio
$k_2$	gyro to pilot lateral control authority ratio
$k_3$	gyro to pilot directional control authority ratio
$L_u, L_v, L_w,$ etc.	aircraft rolling moment derivatives with respect to the variables written as subscripts

$M_u, M_v, M_w,$ etc.	aircraft pitching moment derivatives with respect to the variables written as subscripts
$N_u, N_v, N_w,$ etc.	aircraft yawing moment derivatives with respect to the variables written as subscripts
$R$	damping rate, rad/sec
$t$	time, sec
$(T_Y)_A$	applied control torque to gyro about Y-axis, ft-lb
$T_{\frac{1}{2}}$	the time to half amplitude of aircraft motion, sec
$T_2$	the time to double amplitude of aircraft motion, sec
$u$	aircraft perturbation velocity along the body X-axis, positive forward, ft/sec
$V$	aircraft freestream forward speed, kts
$v$	aircraft perturbation velocity along the body Y-axis, positive to the right, ft/sec
$w$	aircraft perturbation velocity along the body Z-axis, positive down, ft/sec
$X, Y, Z$	aircraft and gyro axes coordinate system
$X_u, X_v,$ etc	aircraft longitudinal force derivatives with respect to the variables written as subscripts
$Y_u, Y_v,$ etc	aircraft side force derivatives with respect to the variables written as subscripts
$Z_u, Z_v,$ etc	aircraft normal force derivatives with respect to the variables written as subscripts

$\alpha$	fuselage pitch attitude, rad
$\beta$	gyro attitude in pitch, rad
$\delta$	gyro attitude in roll, rad
$\eta$	gyro attitude in yaw, rad
$\eta_0$	initial gyro attitude in yaw, rad
$\theta$	aircraft or tilt table pitch attitude, rad
$\theta_{trc}$	tail rotor collective pitch control, rad
$\theta_{trs}$	tail rotor stabilizer pitch control, rad
$\phi$	aircraft roll attitude, rad
$\tau_u$	time constant for aircraft longitudinal velocity response, sec
$\tau_v$	time constant for aircraft lateral velocity response, sec
$\psi$	aircraft yaw attitude, rad
$\psi_p$	gyro phase angle based on input position
$\psi_r$	gyro phase angle based on input rate
$\Omega$	gyro rotational speed, rad/sec
$\omega_y$	gyro input frequency, cps
$(\dot{\phantom{x}})$	time rate derivative, $\frac{d(\phantom{x})}{dt}$



## I. INTRODUCTION

Most of the present-day helicopters require some kind of stability augmentation, which can be provided by either mechanical or electronic stabilization systems.

The mechanical stabilization systems which are known to be quite reliable are generally externally mounted, bulky, and very heavy. These systems provide stabilizing signals to the helicopter control system by means of a gyroscope or a bar system incorporating either aerodynamic or viscous dampers. On the other hand, the electronic stabilization systems which can be light in weight are highly complex, costly and require highly skilled maintenance personnel.

It would be desirable to provide a stability augmentation system that would possess the high reliability characteristics of current mechanical systems and the lightweight characteristics of current electronic devices. As part of a continuing effort to develop such systems, the Dynasciences Corporation has recently demonstrated the feasibility of a lightweight, compact, internally mountable mechanical system known as the Dynagyro. In the Dynagyro design, the inherent problem of miniaturizing the damping of a mechanical system has been bypassed through the use of a coulomb (friction) damped gyro which has been satisfactorily miniaturized.

Under prior contract, a pilot model of the Dynagyro two-axis miniaturized stabilization system has been constructed and extensively bench-tested to evaluate the concept.

On the basis of the promising results obtained from the bench test model of the Dynagyro, the U.S. Army Aviation Materiel Laboratories entered a follow-on contract with Dynasciences Corporation for the construction and reliability evaluation of a flightworthy three-axis mechanical stability augmentation system for helicopters. The system utilizes the two-axis Dynagyro to provide for stability augmentation in pitch and roll in conjunction with the single-axis damped rate gyro to provide for stability augmentation in yaw. Both the Dynagyro and the single-axis Heading Assist Gyro have been subjected to extensive endurance tests (1000 hours for the Dynagyro and

825 hours for the Heading Assist Gyro) to establish the reliability of the overall system. The system characteristics and the results of the reliability evaluation are described in the following section of this report.

## II. SYSTEM DESCRIPTION

The Mechanical Stability Augmentation System (MSAS), shown installed on the test fixture and in exploded views in Figures 1 and 2, respectively, consists of a coulomb-damped two-degree-of-freedom gyroscope (Dynagyro) and a single-axis spring-damped rate gyroscope (Heading Assist).

A detailed description of the Dynagyro concept is presented in Reference 1. The Dynagyro is a hydraulically powered gyroscope spinning at a high rotational speed. Within the gyro mass, and rotating with it, are friction dampers which are hinged to a rotating but nontilting plane. The friction force generated between the dampers and the gyro mass provides a restoring moment tending to return the gyro to its equilibrium position.

The coulomb-damped gyro senses the change in aircraft angular displacement, and provides a corrective input to the aircraft control system through a power boost actuator and mixing linkages.

The Heading Assist Gyroscope is also powered hydraulically. The major components of the drive system consist of a planetary gear transmission and a universal joint. The step-up transmission is capable of providing the gyro spin velocity in excess of 3000 rpm, which is the design limit of the universal joint. Other major components of the Heading Assist Gyro include a torsional leaf spring, for centering, and a viscous damper. Unlike the Dynagyro, the Heading Assist Gyro senses the change in aircraft angular rate rather than the change in aircraft angular attitude. The signal is integrated into the aircraft control system through a control boost actuator and mixing linkages in a manner similar to the Dynagyro.

The integration of the MSAS in a typical helicopter control system is schematically presented in Figure 3. Although this figure represents the MSAS control mixing for the longitudinal cyclic control system, it is equally representative of the lateral and directional control systems. The longitudinal and lateral control inputs, i.e., stability augmentation in aircraft pitch and roll, are provided by the Dynagyro, while the Heading Assist Gyro provides stability augmentation in aircraft yaw.

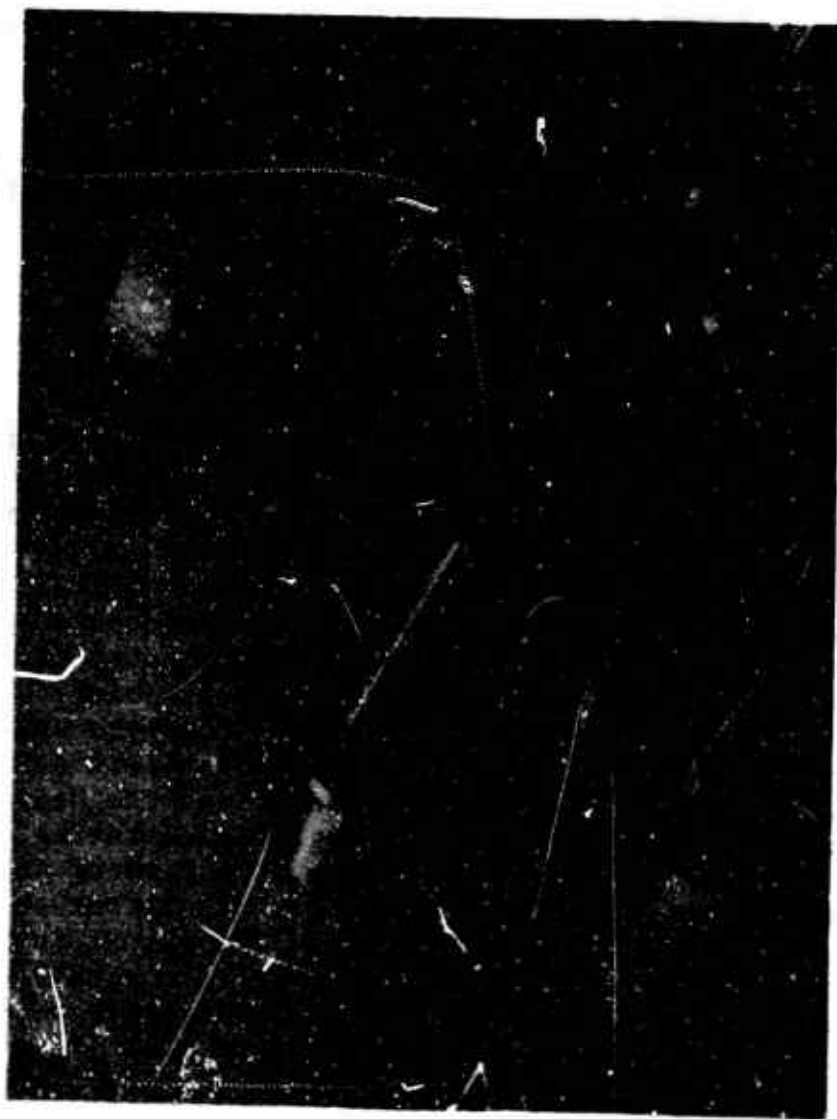


**Figure 1. Reliability Evaluation Test Setup of the MSAS.**



a. Dynagyro



b. Heading Assist Gyro

Figure 2. Exploded View of MSAS Components.

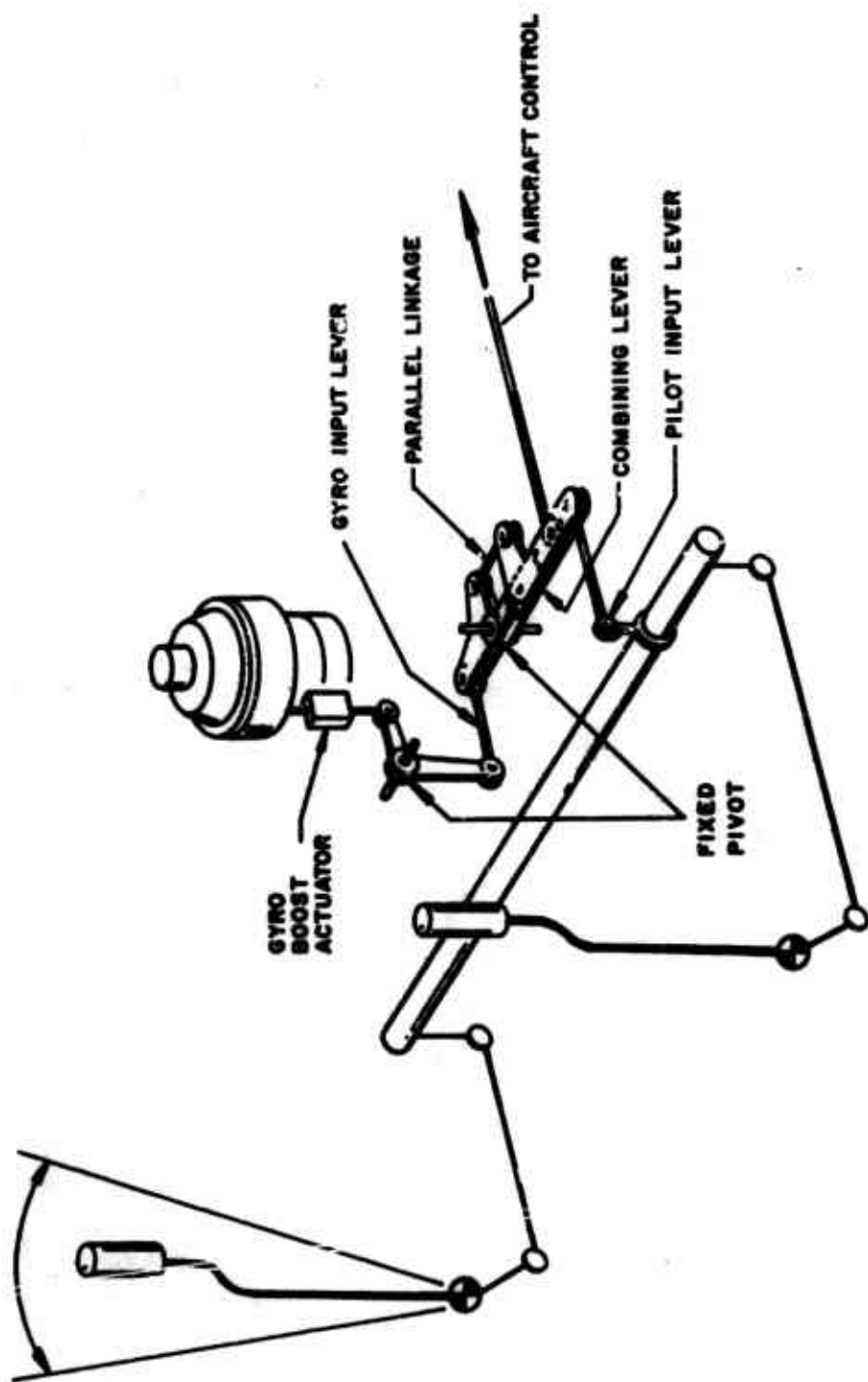


Figure 3. Schematic Representation of MSAS Mixing in a Helicopter Control System.

In order to introduce the gyro control input into the helicopter control system, as shown in Figure 3, it is necessary to reduce the pilot's control to the swash plate such that with the integrated system the sum of pilot and gyro input motion equals the maximum pilot input prior to integration. This is accomplished by modifying the pilot's input lever (see Figure 3) to permit the insertion of a combining lever pivoted about a fixed point. In conjunction with the combining lever, a parallelogram linkage is provided which mixes the gyro input with the pilot input. With this configuration, an input by the gyro, with the pilot stick fixed, moves the output lever through the parallelogram linkage. Conversely, with the gyro fixed, an input by the pilot moves the output lever by an amount proportional to the pilot's authority ratio. The ratio of gyro to pilot control motion, as well as the damping requirements on the MSAS, is determined by an analog simulation of the coupled aircraft-controller system.

The specifications of the MSAS are summarized in Table I.

**TABLE I****MSAS SPECIFICATIONS**

<b>Item</b>	<b>Dynagyro</b>	<b>Heading Assist Gyro</b>
<b>Weight</b>	<b>16.3 lb</b>	<b>14.5 lb</b>
<b>Size</b>	<b>9.5 in. x 9.5 in. x 12.5 in.</b>	<b>6.5 in. x 8.25 in. x 12.5 in.</b>
<b>RPM</b>	<b>4000</b>	<b>9700</b>
<b>Angular Momentum</b>	<b>92 in-lb-sec</b>	<b>100 in-lb-sec</b>
<b>Damping</b>	<b>.008 rad/sec</b>	<b>175 in-lb/rad/sec</b>
<b>Spring Rate</b>		<b>50 in-lb-rad</b>
<b>Fluid Flow</b>	<b>1.12 GPM</b>	<b>6.62 GPM</b>
<b>Pressure</b>	<b>1500 psi</b>	<b>1500 psi</b>
<b>Power Requirement</b>	<b>1.0 HP</b>	<b>.54 HP</b>



### III. ANALOG COMPUTER SIMULATION OF THE HUGHES 269-A HELICOPTER EQUIPPED WITH THE NSAS

#### A. ANALOG COMPUTER PROGRAM

The design criteria of the NSAS were established using the results of an analog computer study conducted as part of this program. This study was based on the integration of the NSAS with a 269-A helicopter intended to be the test vehicle for a follow-on flight test evaluation program.

The dynamic analog simulation was conducted on a Pace 221 computer. The computer scaled equations of motion of the Hughes 269-A helicopter equipped with the NSAS and the equation of motion of the Pyrogyro and Heading Assist Gyro are as follows:

#### 1. Longitudinal Mode

$$\ddot{\theta} = -\frac{N_2}{N_5}\dot{\theta} - \frac{N_2}{N_5}\theta - \frac{10 N_2}{N_5} \left[ \frac{u}{15} \right] \\ - \frac{10 N_2}{N_5} \left[ \frac{u}{15} \right] - \frac{N_{21}}{N_5} \left\{ J_1 (\dot{\beta}_{1D}) + (\beta_{1D}) \right\} \quad (1)$$

$$\frac{\ddot{\theta}}{10} = -\frac{K_2}{10 K_5} \dot{\theta} - \frac{K_2}{10 K_5} \theta - \frac{K_2}{K_5} \left[ \frac{u}{15} \right]$$

$$\frac{K_2}{K_5} \left[ \frac{u}{15} \right] - \frac{K_{21}}{10 K_5} \left\{ J_1 (\dot{\beta}_{1D}) + (\beta_{1D}) \right\} \quad (2)$$

$$\begin{aligned} \frac{\dot{w}}{10} = & - \frac{Z_{\dot{\theta}}}{10 Z_w} \dot{\theta} - \frac{Z_{\theta}}{10 Z_w} \theta - \frac{Z_u}{Z_w} \left[ \frac{u}{10} \right] \\ & - \frac{Z_w}{Z_w} \left[ \frac{w}{10} \right] - \frac{Z_{B1}}{10 Z_w} \left\{ J_1 (B_{1c}) + (B_{1s}) \right\} \end{aligned} \quad (3)$$

$$\dot{B}_{1s} = -k_1 \dot{\theta} - k_2 R \frac{B_{1s}}{|B_{1s}|} \quad (4)$$

## 2. Lateral Directional Mode

$$\begin{aligned} \ddot{\psi} = & - \frac{N_{\dot{\psi}}}{N_{\ddot{\psi}}} \dot{\psi} - \frac{N_{\psi}}{N_{\ddot{\psi}}} \psi - \frac{10 N_V}{N_{\ddot{\psi}}} \left[ \frac{v}{10} \right] \\ & - \frac{N_{A1}}{N_{\ddot{\psi}}} \left\{ J_2 (A_{1c}) + (A_{1s}) \right\} \\ & - \frac{N_{\theta 1}}{N_{\ddot{\psi}}} \left\{ J_3 (\theta_{1c}) + (\theta_{1s}) \right\} \end{aligned} \quad (5)$$

$$\begin{aligned} \ddot{\phi} = & - \frac{L_{\dot{\psi}}}{L_{\ddot{\phi}}} \dot{\psi} - \frac{L_{\psi}}{L_{\ddot{\phi}}} \psi - \frac{10 L_V}{L_{\ddot{\phi}}} \left[ \frac{v}{10} \right] \\ & - \frac{L_{A1}}{L_{\ddot{\phi}}} \left\{ J_2 (A_{1c}) + (A_{1s}) \right\} \\ & - \frac{L_{\theta 1}}{L_{\ddot{\phi}}} \left\{ J_3 (\theta_{1c}) + (\theta_{1s}) \right\} \end{aligned} \quad (6)$$

$$\frac{\dot{V}}{10} = - \frac{Y_{\dot{V}}}{10 Y_{\dot{V}}} \dot{\psi} - \frac{Y_{\psi}}{10 Y_{\dot{V}}} \psi - \frac{Y_{\dot{\phi}}}{10 Y_{\dot{V}}} \dot{\phi} - \frac{Y_{\phi}}{10 Y_{\dot{V}}} \phi$$

$$\frac{Y_{\theta_1}}{10 Y_{\dot{V}}} \{J_2(A_{1c}) + (A_{1s})\} \frac{Y_{\theta_1}}{10 Y_{\dot{V}}} \{J_3(\theta_{trc}) + (\theta_{trs})\} \quad (7)$$

$$\dot{A}_{1s} = - k_2 \dot{\phi} - k_{2R} \frac{A_{1s}}{|A_{1s}|} \quad (8)$$

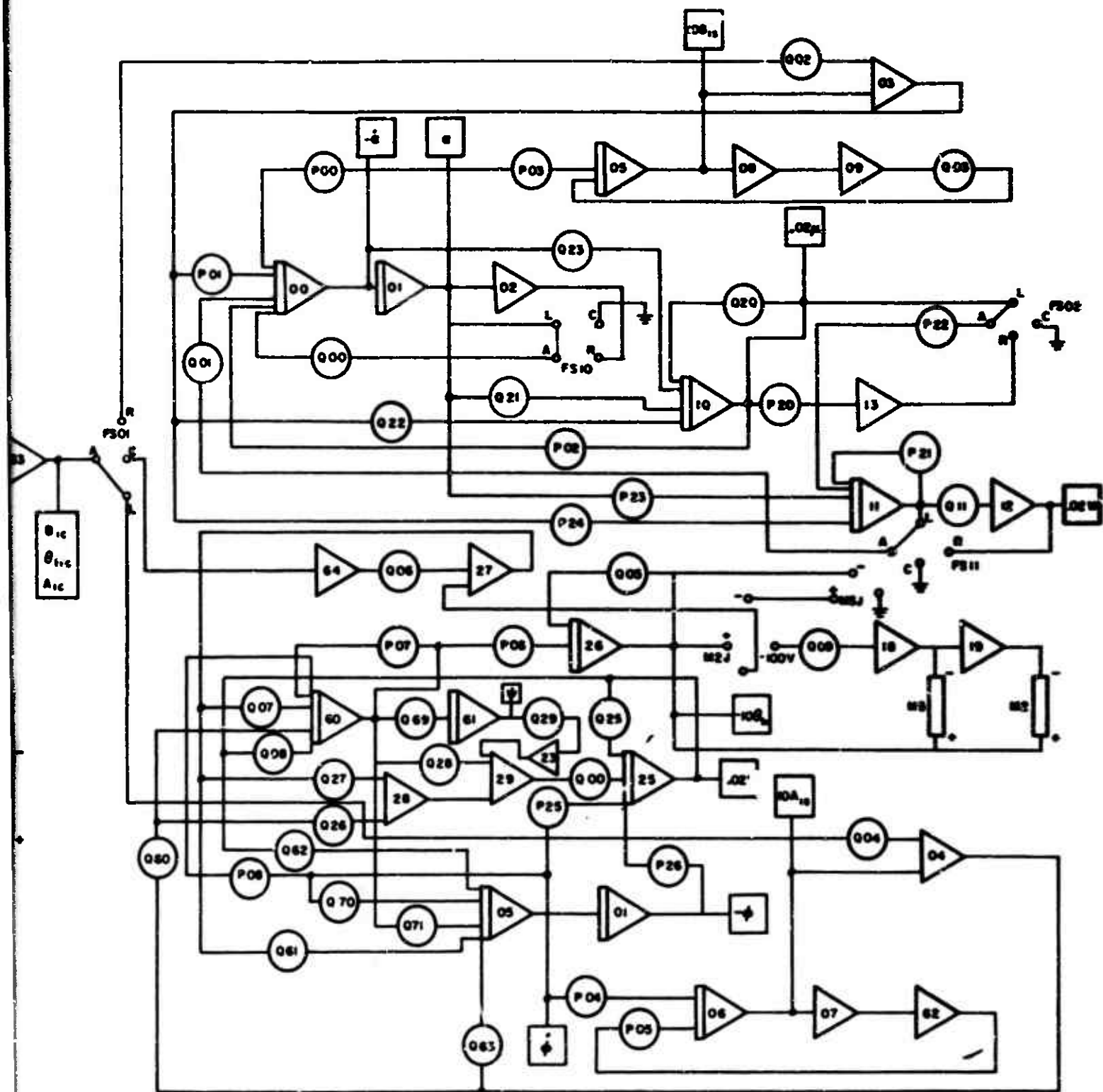
$$\dot{\theta}_{trs} = - k_3 \frac{I_s \Omega}{C_D} \dot{\psi} - \frac{k_s}{C_D} \theta_{trs} \quad (9)$$

The computer schematic of the equation of motion is presented in Figure 4. The numerical values of helicopter stability derivatives used in the equations of motion were evaluated using the theoretical methods of Reference 2. These values which are herein presented in Table II, apply to the 269-A helicopter equipped with the MSAS.

Since the 269-A helicopter has been shown to possess neutral stability characteristics at high forward speeds, the analog simulation was performed for a half-tail configuration. The reduction in tail surface area of the helicopter provided for a more effective evaluation of the stability augmentation characteristics of the MSAS at high forward speeds.

Although the present analog simulation study specifically applies to the 269-A helicopter (including a half-tail configuration at high speeds), the basic design of the MSAS is applicable to a wide range of helicopter configurations. The application of the MSAS to a different helicopter requires minor modifications in the damping rates of the system and in the degree of mixing ratios of the gyro control inputs.





Schematic.

P

**TABLE II**  
**TOTAL STABILITY DERIVATIVES**  
**(a) Hovering**

Variable	X	Y	N	L	H
$\delta$	-1535	-	-	-	-
$\dot{\delta}$	83.72	-	-545.17	-	-
$\ddot{\delta}$	-	-	-373	-	-
$u$	-0.9671	-	5.657	-	-
$\dot{u}$	-47.671	-	-	-	-
$v$	-	-1.618	-	-6.913	8.061
$\dot{v}$	-	-47.67	-	-	-
$\phi$	-	1535	-	-	-
$\dot{\phi}$	-	-	-	-536.27	47.80
$\ddot{\phi}$	-	-	-	-219	-
$\dot{\psi}$	-	8.406	-	14.79	-161.16
$\ddot{\psi}$	-	-	-	-	-252
$B_{\delta} B_{\epsilon}$	1535	-	-8915.8	-	-
$A_{\delta} A_{\epsilon}$	-	1535	-	8915.8	-640.1
$B_{\delta} B_{\eta}$	-	-559.1	-	-861.0	7995.0

**TABLE II - Continued**  
**(b) V = 35 knots**

Variable	X	Y	Z	L	M	N
$\alpha$	-1530.7	-	1823.8	-	-148.52	-
$\dot{\alpha}$	-	-	-	-	-622.61	-
$\ddot{\alpha}$	-	-	-	-	-373	-
$u$	-1.79	-	47.11	-	19.003	-
$\dot{u}$	-47.67	-	-	-	-	-
$v$	-	-1.78	-	-6.409	-	13.15
$\dot{v}$	-	-47.67	-	-	-	-
$\phi$	-	1535	-	-	-	-
$\dot{\phi}$	-	-310.56	-	-583.43	-	62.74
$\ddot{\phi}$	-	-	-	-219	-	-
$\psi$	-	-115.68	-	-	-	-
$\dot{\psi}$	-	-2804.2	-	21.79	-	-212.8
$\ddot{\psi}$	-	-	-	-	-	-252
$B_{ls}, B_{lc}$	1530.7	-	-1823.8	-	-8760.2	-
$w$	-	-	-30.86	-	2.515	-
$\dot{w}$	-	-	-47.67	-	-	-
$A_{ls}, A_{lc}$	-	1535	-	8915.8	-	-640.1
$\theta_{lrs}, \theta_{lrc}$	-	-627.0	-	-965.7	-	8966.9

TABLE II - Continued  
(c)  $V = 70$  knots

Variable	X	Y	Z	L	M	N
$\alpha$	-1481	-	4168.7	-	-180.62	-
$\dot{\alpha}$					-569.96	
$\ddot{\alpha}$					-373	
u	-2.20	-	-0.293	-	11.68	-
$\dot{u}$	-47.67	-	-	-	-	-
v	-	-2.045	-	-6.85	-	16.22
$\dot{v}$	-	-47.67	-	-	-	-
$\phi$	-	1535	-	-	-	-
$\dot{\phi}$	-	-621.78	-	-584.26	-	73.086
$\ddot{\phi}$	-	-	-	-219	-	-
$\psi$	-	-142.76	-	-	-	-
$\dot{\psi}$	-	-5608.2	-	27.65	-	-273.9
$\ddot{\psi}$	-	-	-	-	-	-252
$B_{1s}, B_{1c}$	1481	-	-4168.7	-	-8565.8	-
$A_{1s}, A_{1c}$	-	1535	-	8915.8	-	-640.1
w	-	-	-35.33	-	1.53	-
$\dot{w}$	-	-	-47.67	-	-	-



## B. ANALOG COMPUTER RESULTS

Typical analog simulation results showing the response of the MSAS-equipped 269-A helicopter are presented in Figures 5, 6 and 7 for hover, 35 and 70 knots, respectively. Figures 5(a) and 5(b) present analog time histories of the longitudinal and lateral responses of the unstabilized 269-A helicopter, while Figures 5(c) and 5(d) present the longitudinal and lateral responses of the 269-A equipped with the MSAS. These responses were excited by 1-second pulse inputs of 1-inch stick deflection of the longitudinal and lateral cyclic controls  $B_{1c}$  and  $A_{1c}$ , respectively.

Examining Figures 5(a) through 5(d), it can be seen that in hover the unstabilized 269-A helicopter exhibits highly divergent oscillations both in the longitudinal and lateral degrees of freedom; whereas, the MSAS stabilized helicopter exhibits completely stable characteristics. Similar trends in overall stabilization effectiveness of the MSAS can be seen in Figures 6(a) through 6(d) and Figures 7(a) through 7(d) for 35 and 70 knots, respectively.

## C. PARAMETRIC EVALUATION

In order to determine the optimum MSAS configuration for the Hughes 269-A helicopter, a parametric evaluation was performed by varying the geometric parameters of both the Dynagyro and the Heading Assist Gyro. The parameters varied were the Dynagyro damping rate  $R$ , the Heading Assist Gyro damper/spring constant ratio  $k_s/C_D$ , and the pilot to gyro authority ratio.

Figures 8 through 18 show the effect of variation of the stabilizer of the Dynagyro and the Heading Assist Gyro on the dynamic stability characteristics of the 269-A helicopter. Specifically, Figures 8, 9, and 10 show the effect of the Dynagyro damping rate on the helicopter time to half amplitude in pitch and the period of oscillation for different pilot to gyro authority ratios at hover, 35 and 70 knots, respectively.

Figures 11, 12, and 13 show the effect of the Dynagyro damping rate on the helicopter time to half amplitude in roll for different pilot to gyro authority ratios at hover, 35 knots and 70 knots, respectively.

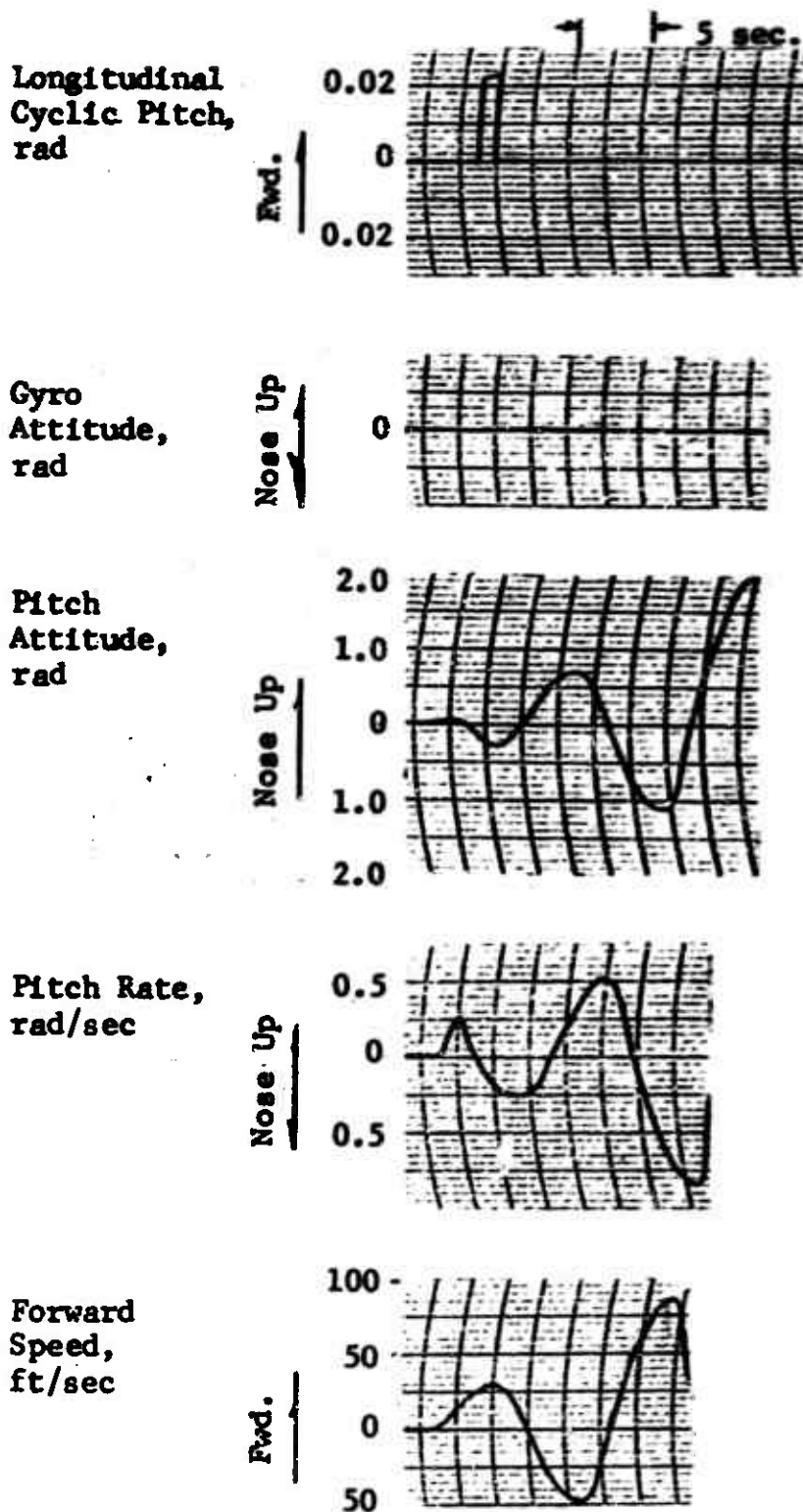


Figure 5. Response of the 269-A Helicopter (Half-Tail) to a Pulse Control Input (Hover).  
(a) Longitudinal - Unstabilized

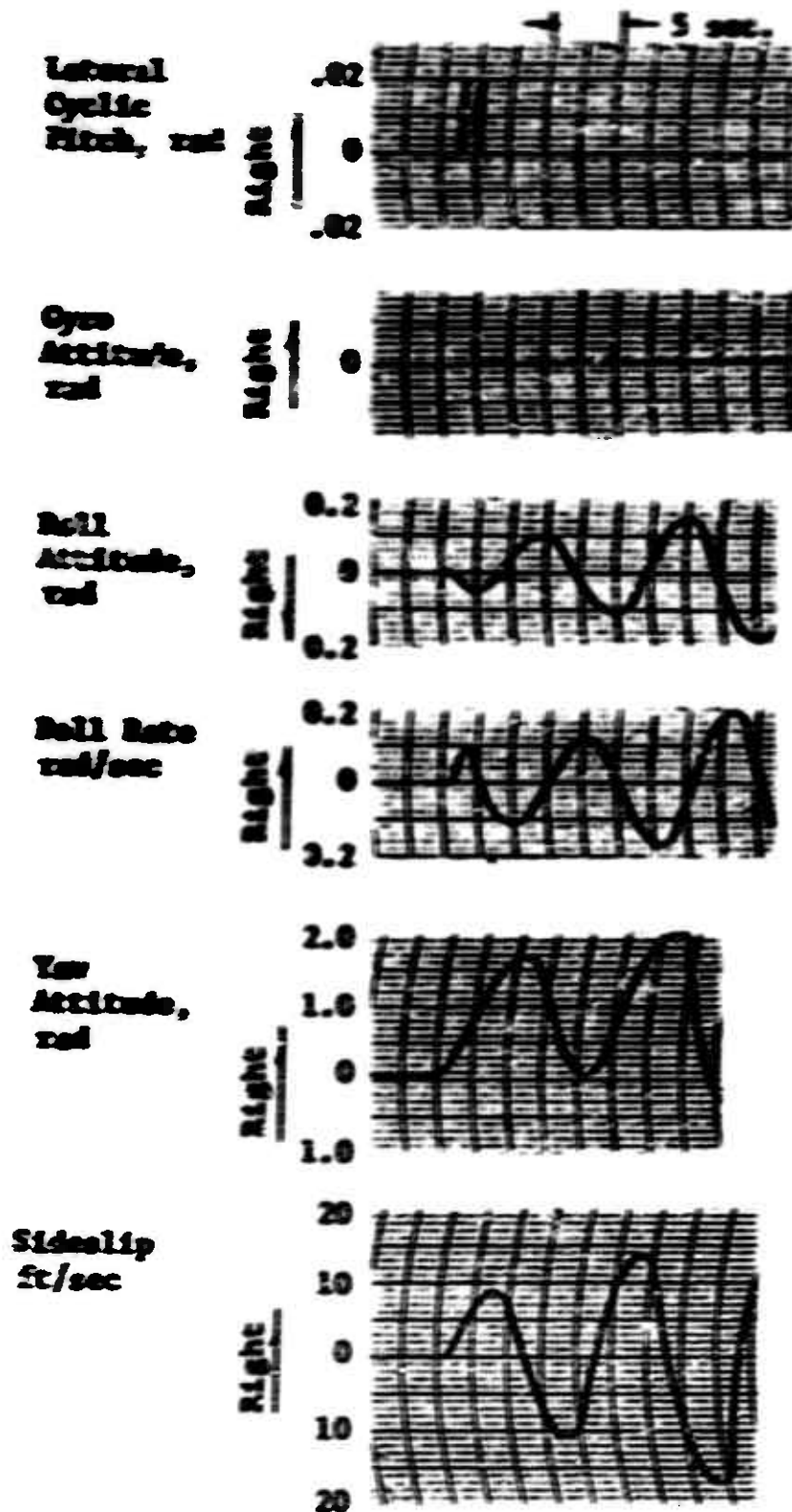
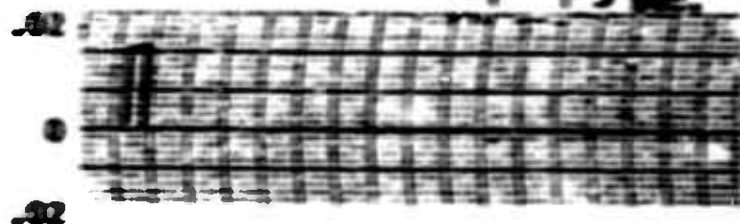


Figure 5. (Continued),  
(b) Lateral - Unstabilized

$k_1$	= 0.10
$k_2$	= 0.10
$k_3$	= 0.10
$k_4$	= 0.0075
$k_5/k_6$	= 0.3

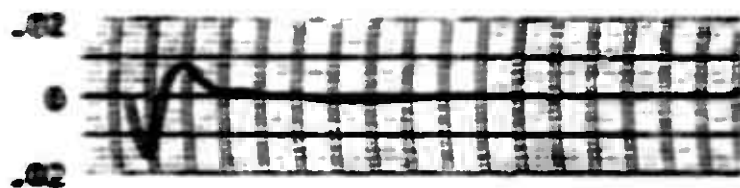
Longitudinal  
Cyclic  
Pitch, rad

Rad.



Cyc  
Attitude,  
rad

Nose Up



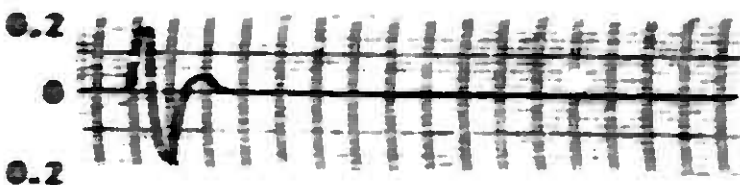
Pitch  
Attitude,  
rad

Nose Up



Pitch Rate,  
rad/sec

Nose Up



Forward  
Speed,  
ft/sec

Rad.

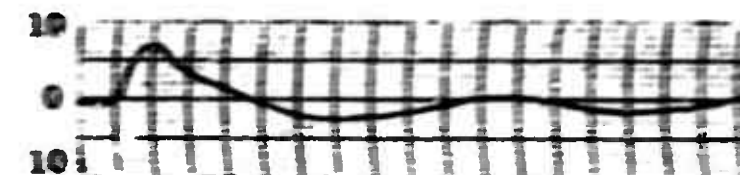


Figure 5. (Continued).

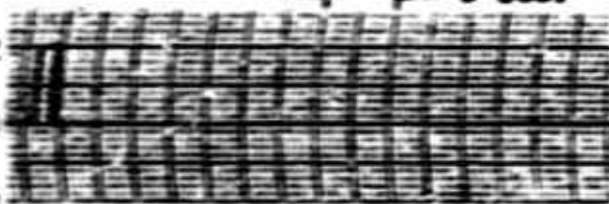
(c) Longitudinal - Stabilized

Parameters:  $k_1 = 0.10$ ;  $k_2 = 0.10$ ;  $k_3 = 0.20$ ;  
 $z = 0.0075$ ;  $k_4/C_2 = 0.3$

Lateral  
 Cyclic Pitch,  
 rad

Right

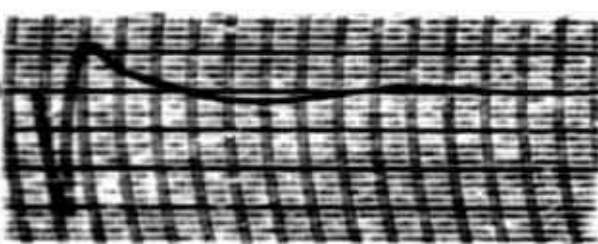
.02  
 0  
 .02



Cyc  
 Amplitude,  
 rad

Right

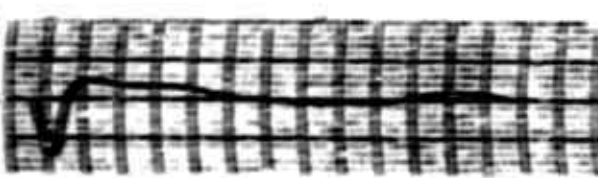
.02  
 0  
 .02



Roll  
 Amplitude,  
 rad

Right

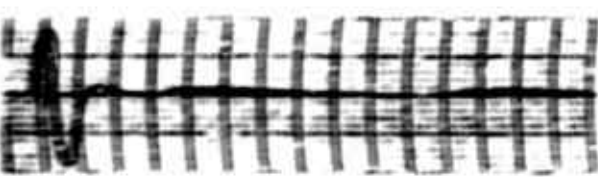
0.2  
 0  
 0.2



Roll Rate,  
 rad/sec

Right

0.2  
 0  
 0.2



Yaw  
 Amplitude,  
 rad

Right

0.2  
 0  
 0.2



Sideslip  
 ft./sec

Right

10  
 0  
 10

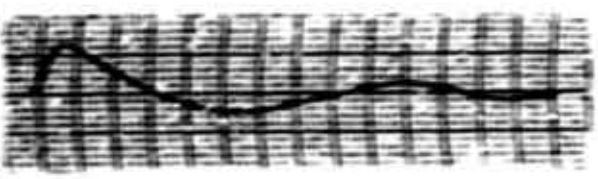


Figure 5. (Continued).  
 (c) Lateral - Stabilized

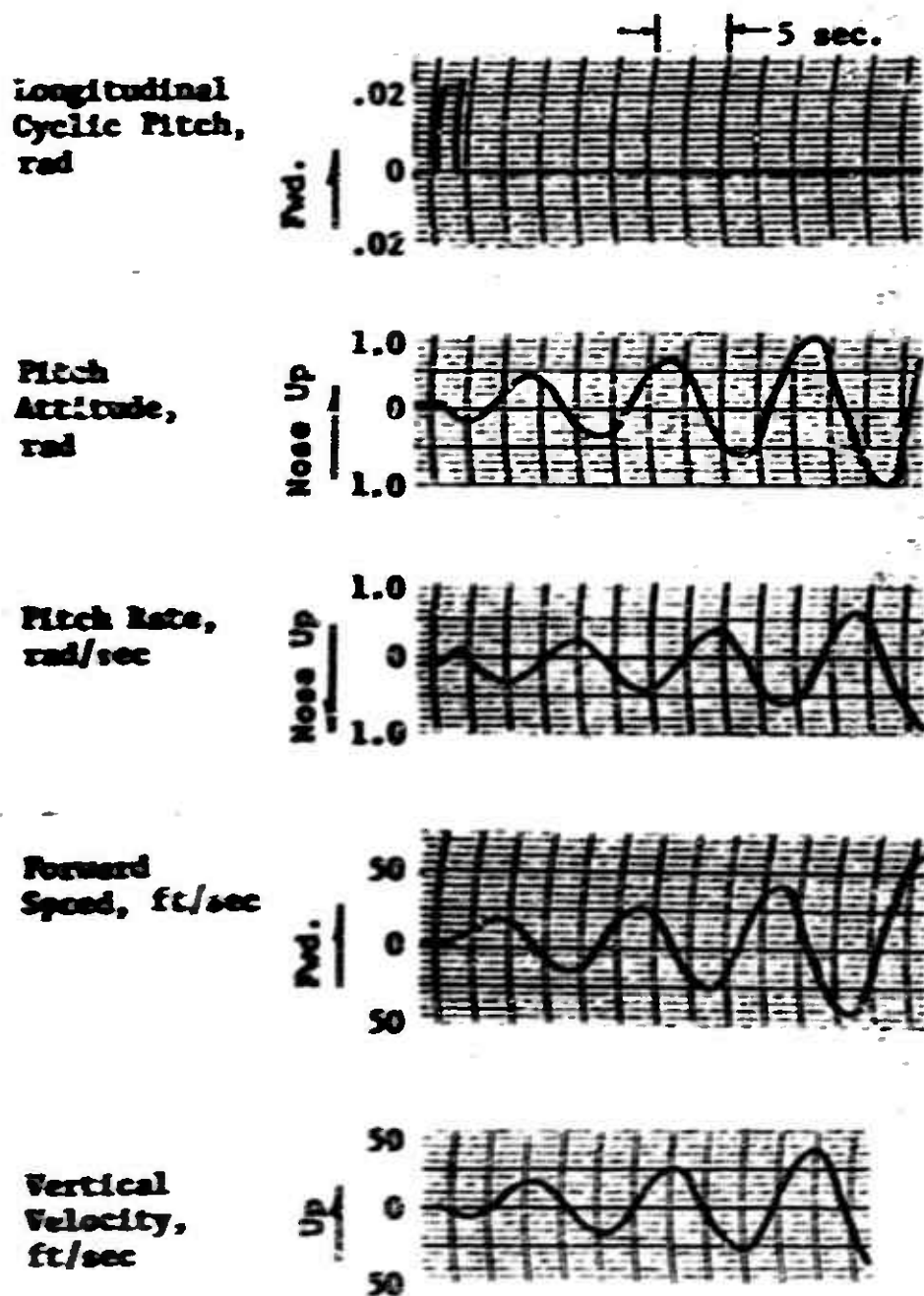


Figure 6. Response of the 269-A Helicopter (Half-Tail) to a Pulse Control Input (35 Knots).  
(a) Longitudinal - Unstabilized

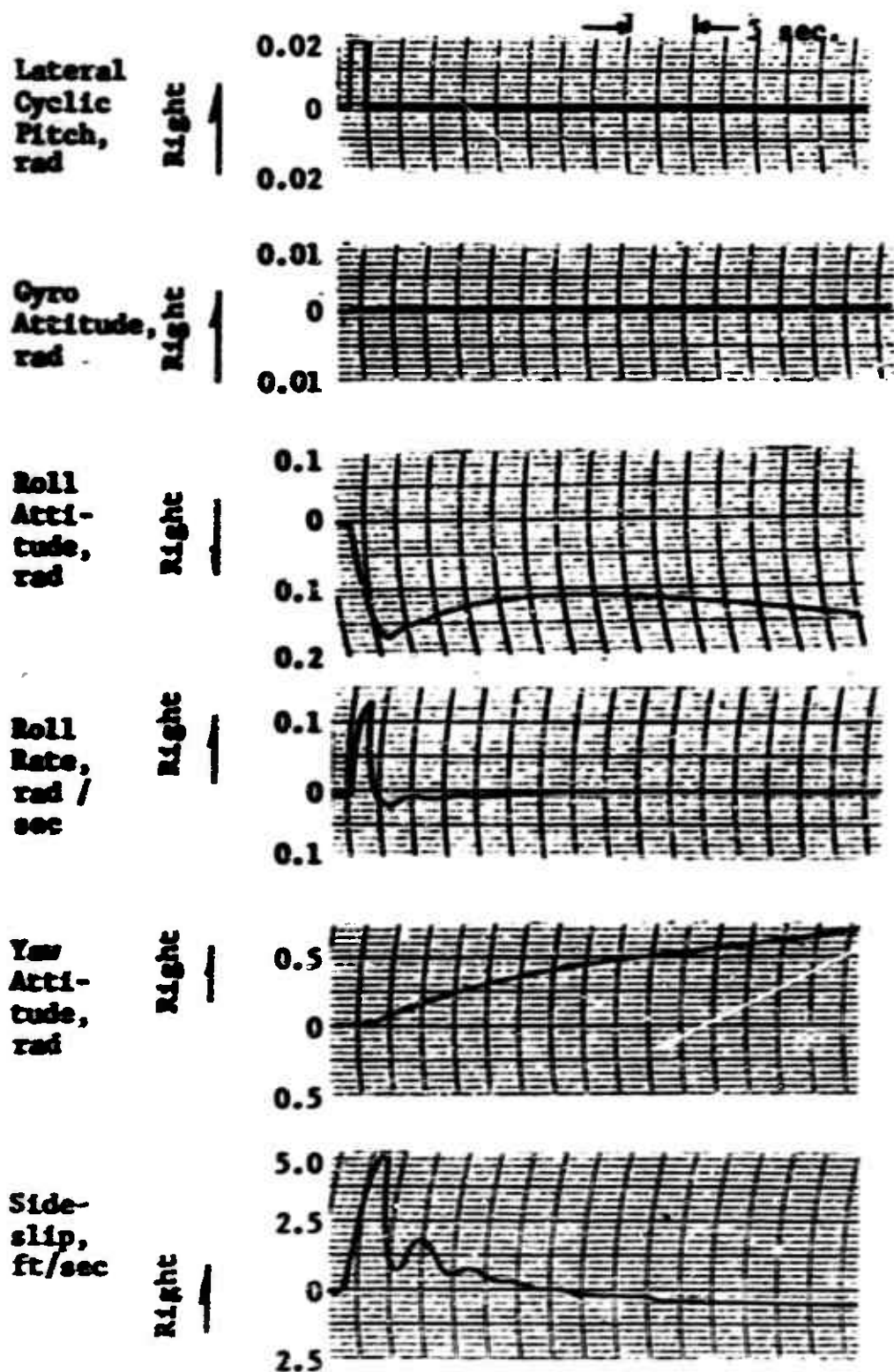


Figure 6. (Continued).  
 (b) Lateral - Unstabilized



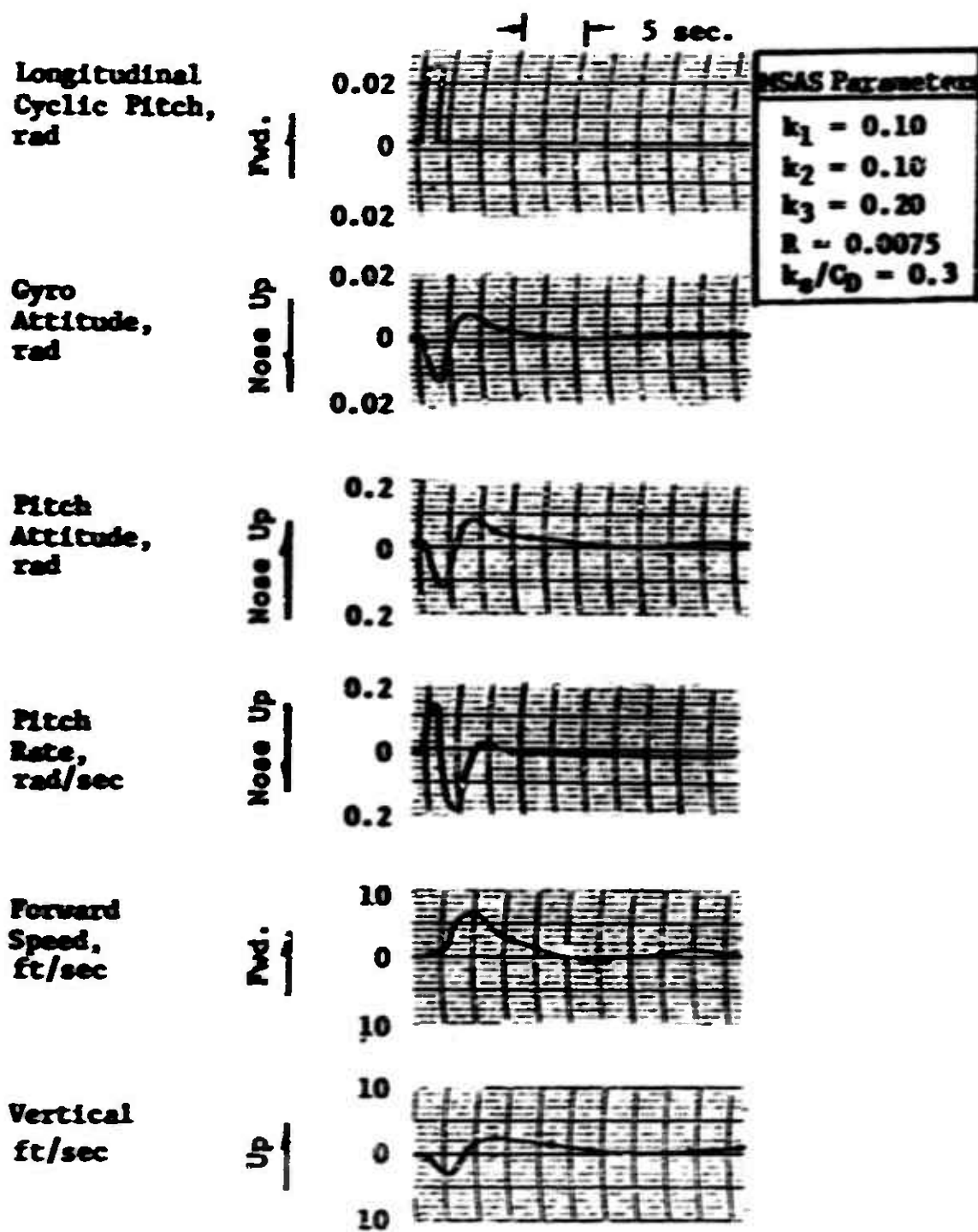


Figure 6. (Continued).

(c) Longitudinal - Stabilized



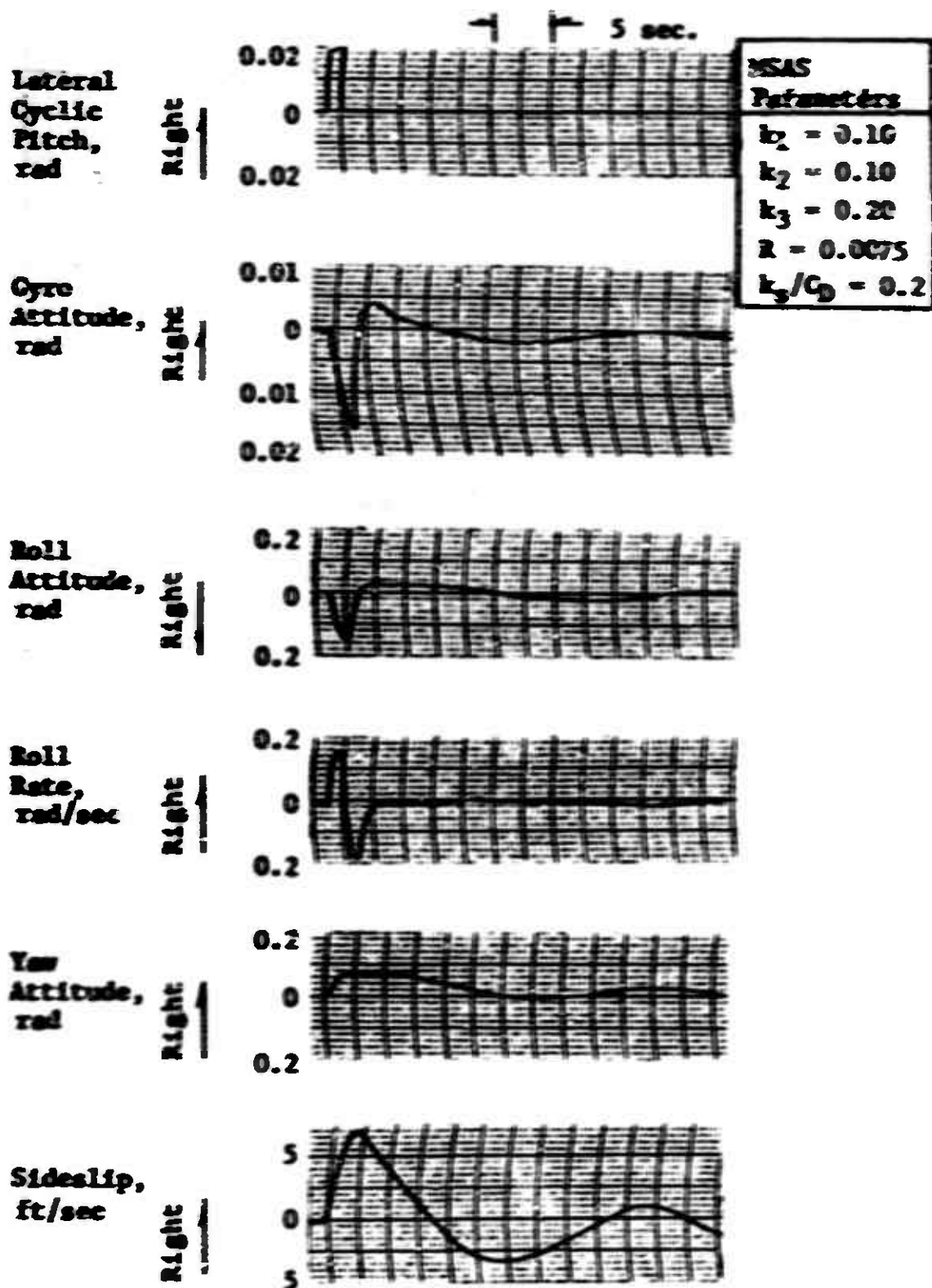


Figure 6. (Continued).  
(d) Lateral - Stabilized

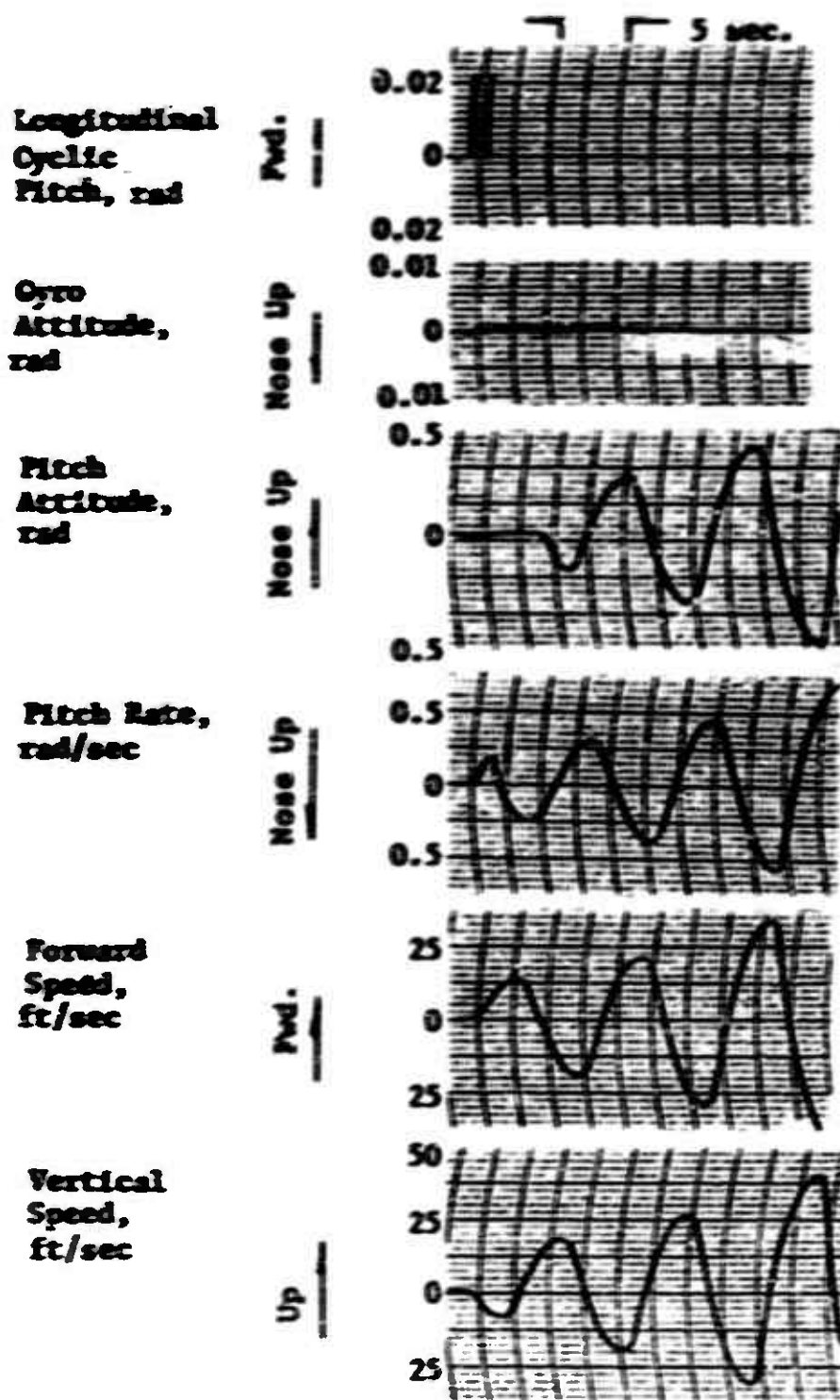


Figure 7. Response of the 269-A Helicopter (Half-Tail) to a Pulse Control Input (70 Knots).  
(a) Longitudinal - Unstabilized

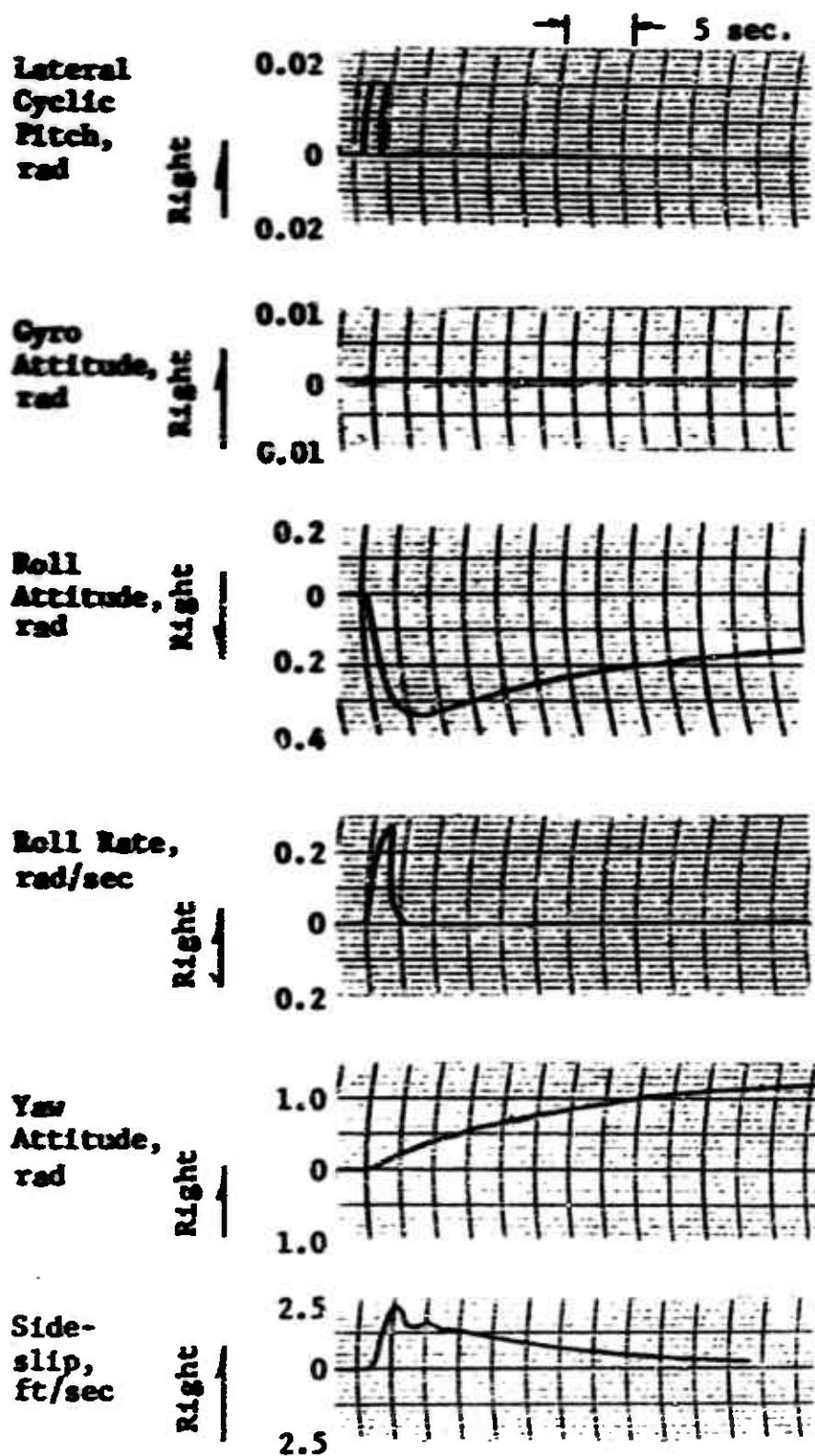


Figure 7. (Continued).  
(b) Lateral - Unstabilized

FSAS Parameters:  $k_1 = 0.10$ ;  $k_2 = 0.10$ ;  $k_3 = 0.20$ ;  
 $R = 0.0075 k_R / C_D = 0.3$

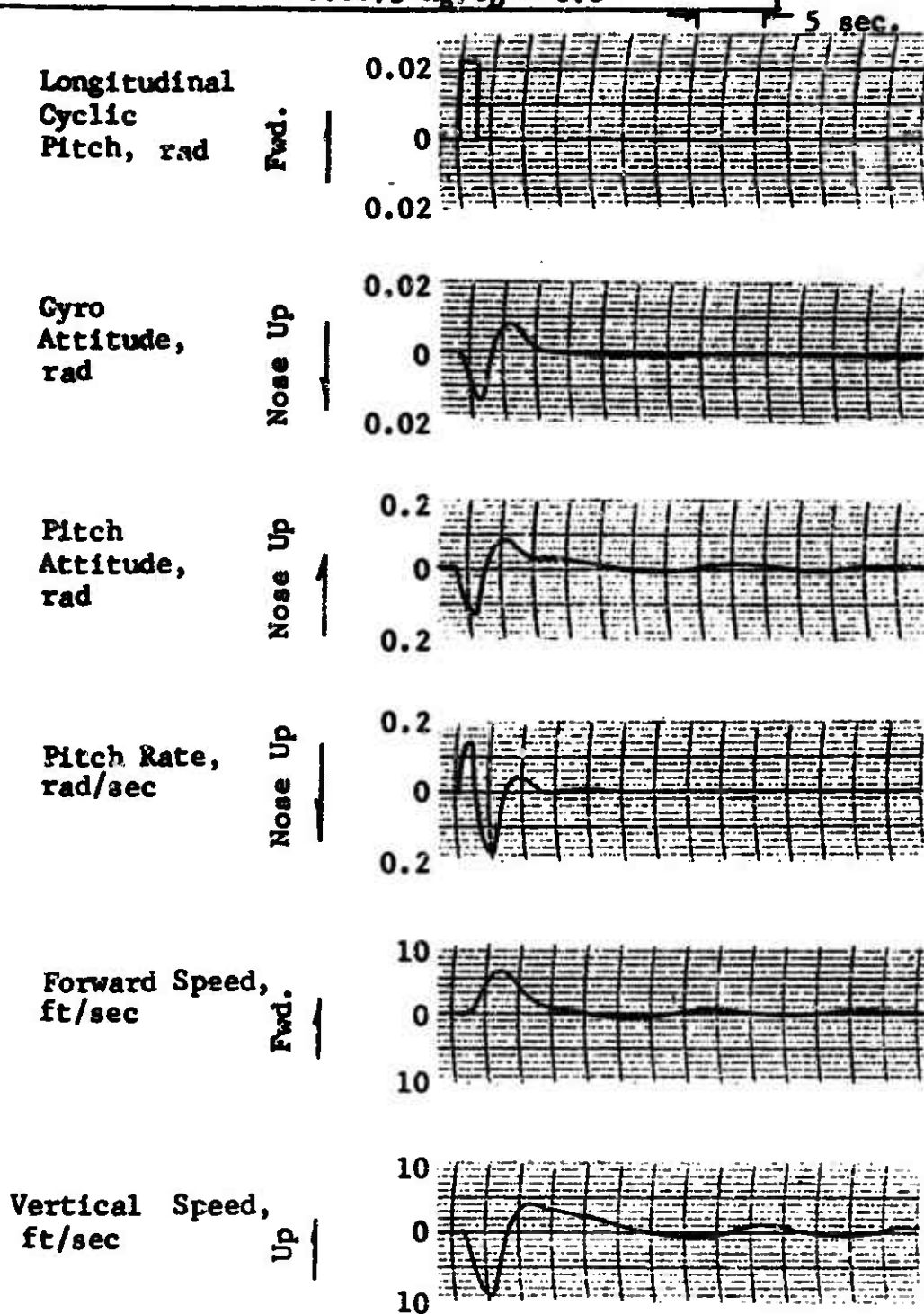


Figure 7. (Continued).  
(c) Longitudinal - Stabilized

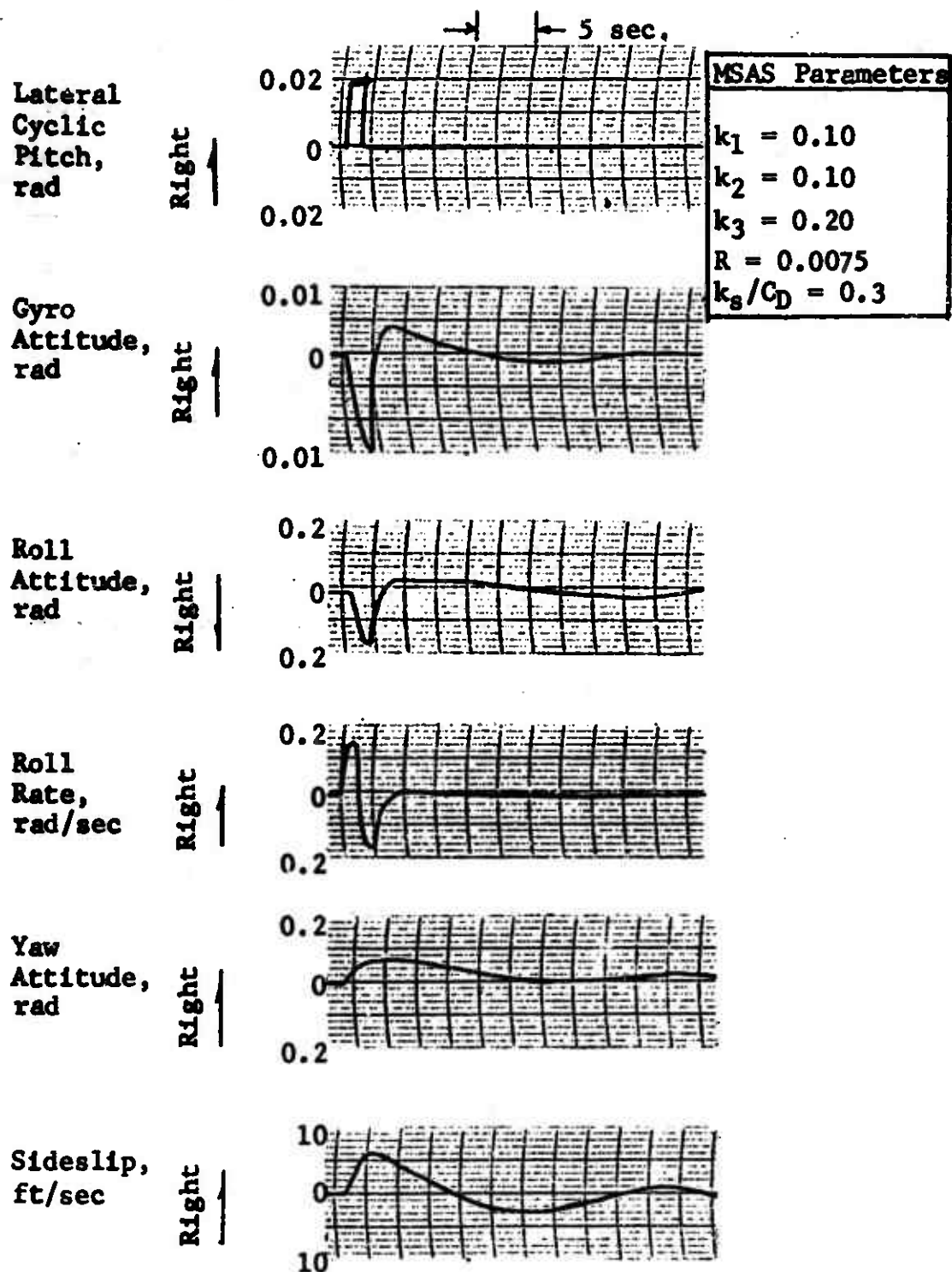


Figure 7. (Continued).

(d) Lateral - Stabilized

SYM	L <sub>1</sub>
O	0.05
□	0.10
Δ	0.15

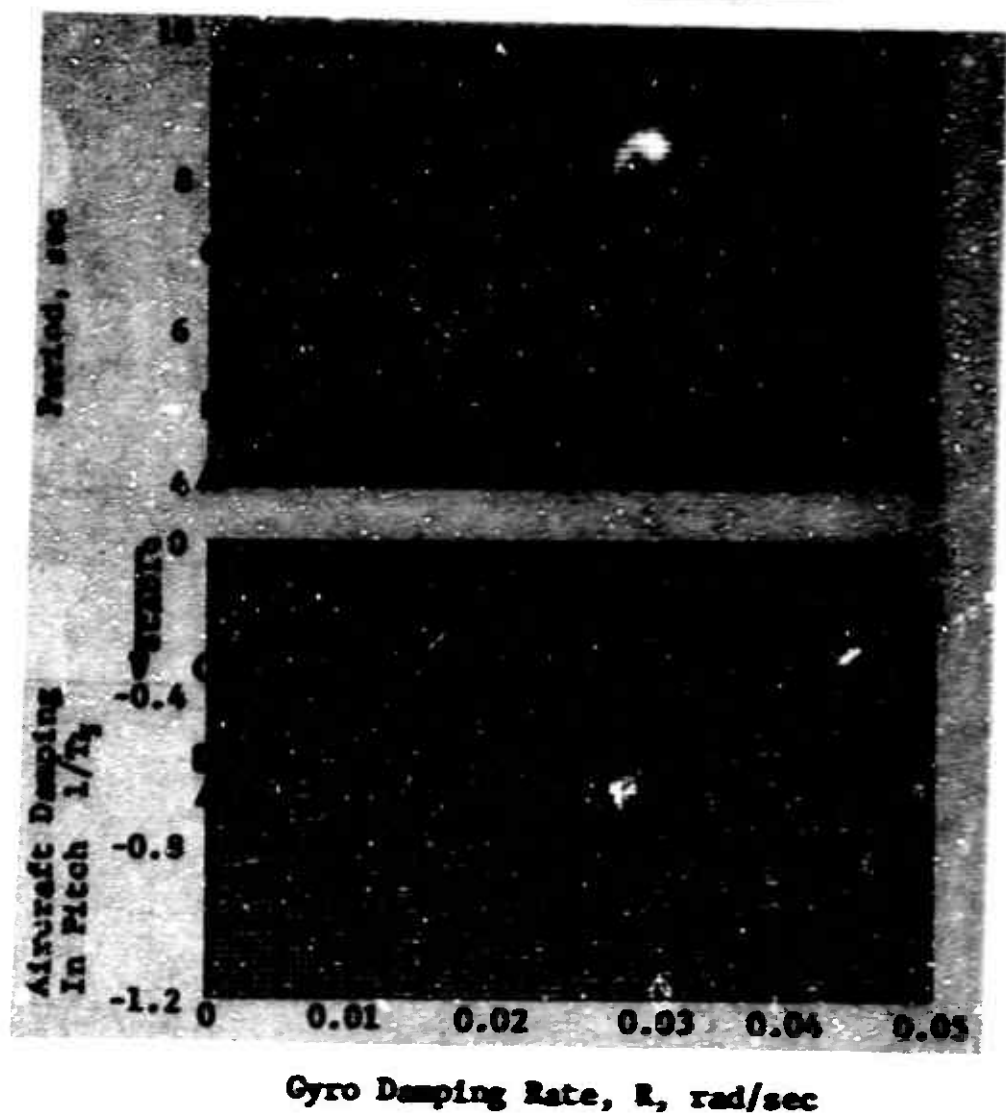
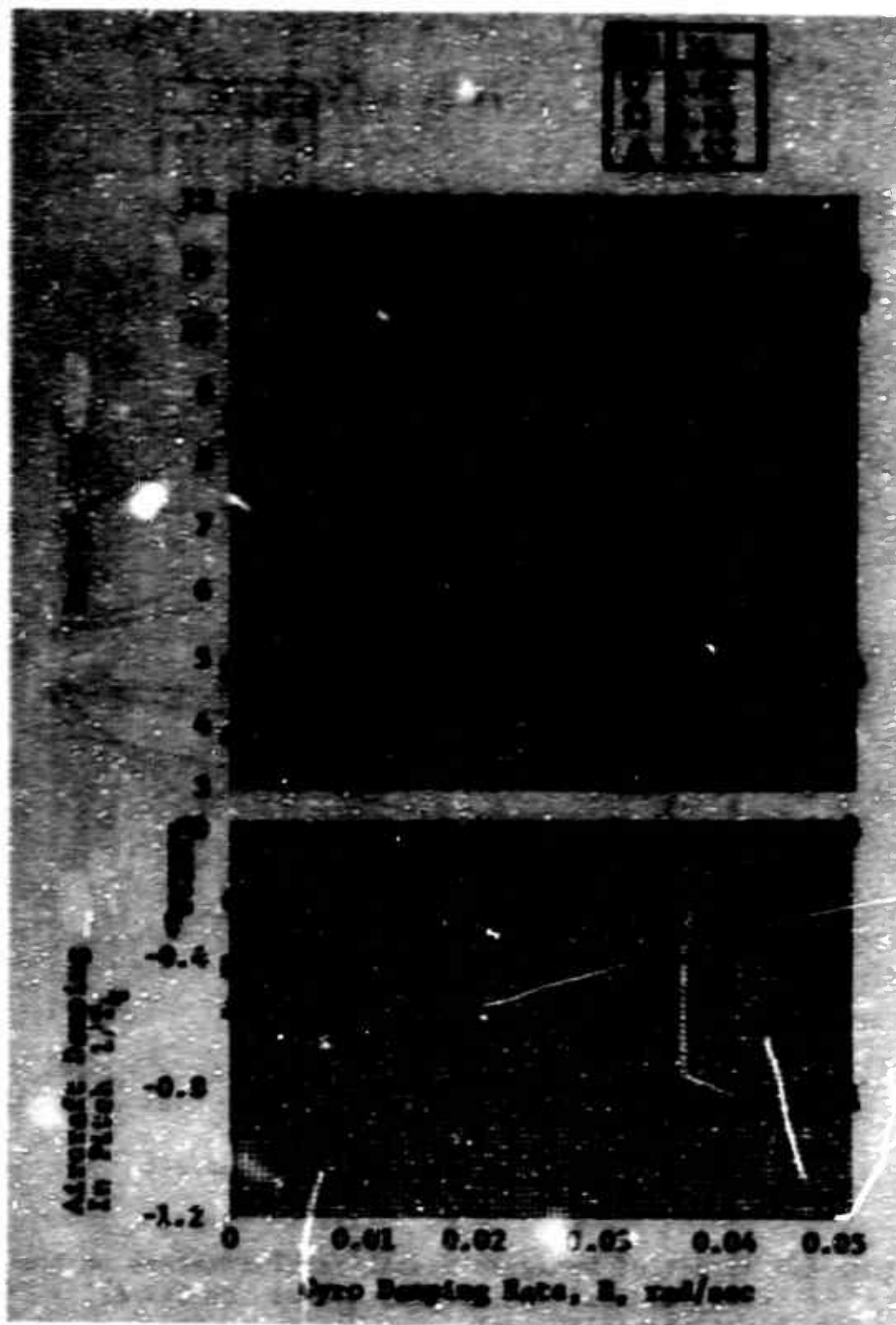


Figure 8. Effect of Dynagyro Stabilizer Parameters on the Longitudinal Characteristics of the 269-A Helicopter (Hover).



**Figure 9. Effect of Dycgyro Stabilizer Parameters on the Longitudinal Characteristics of the 269-A Helicopter (35 Knots).**



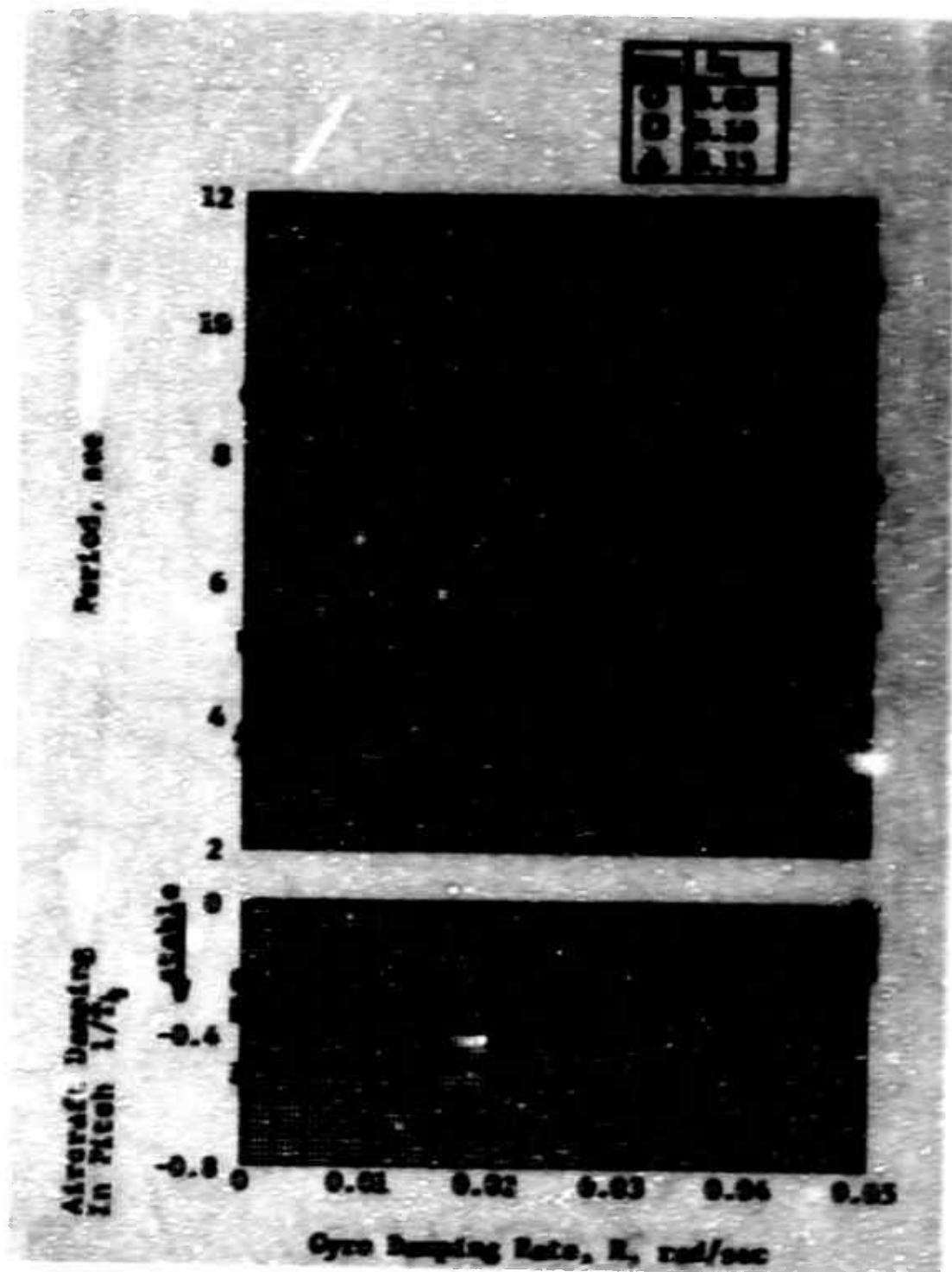


Figure 10. Effect of Dynagyro Stabilizer Parameters on the Longitudinal Characteristics of the 259-A Helicopter (70 Knots).



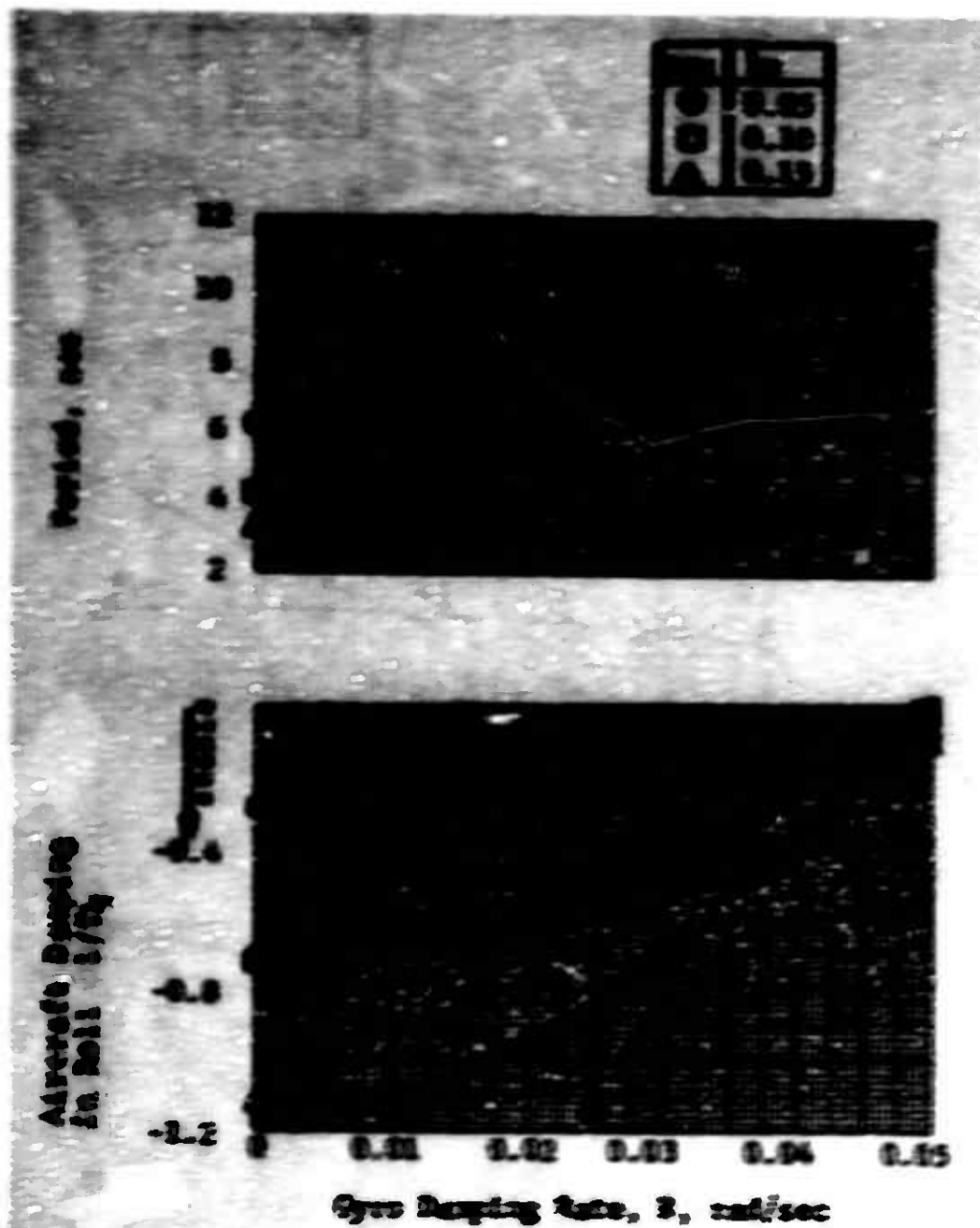
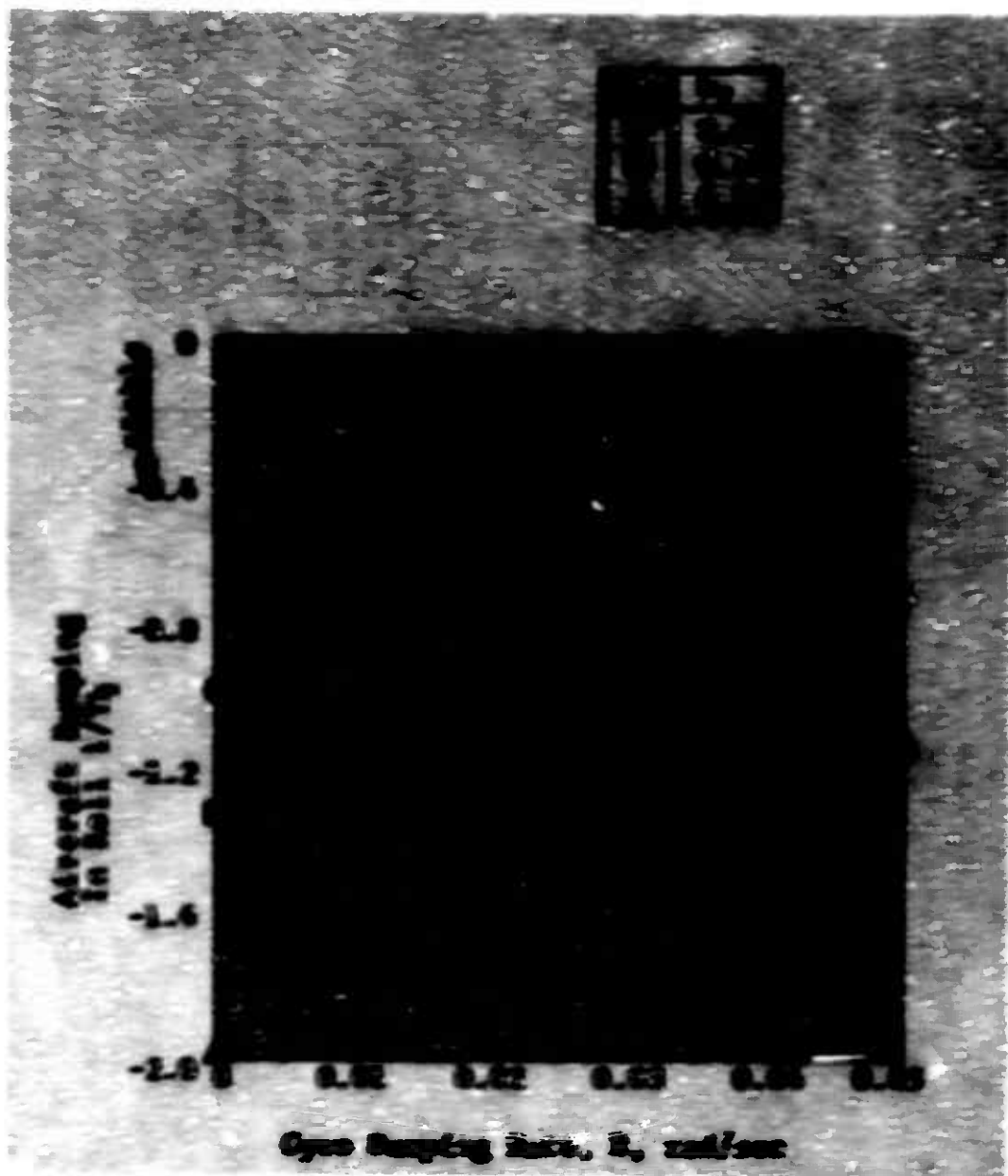
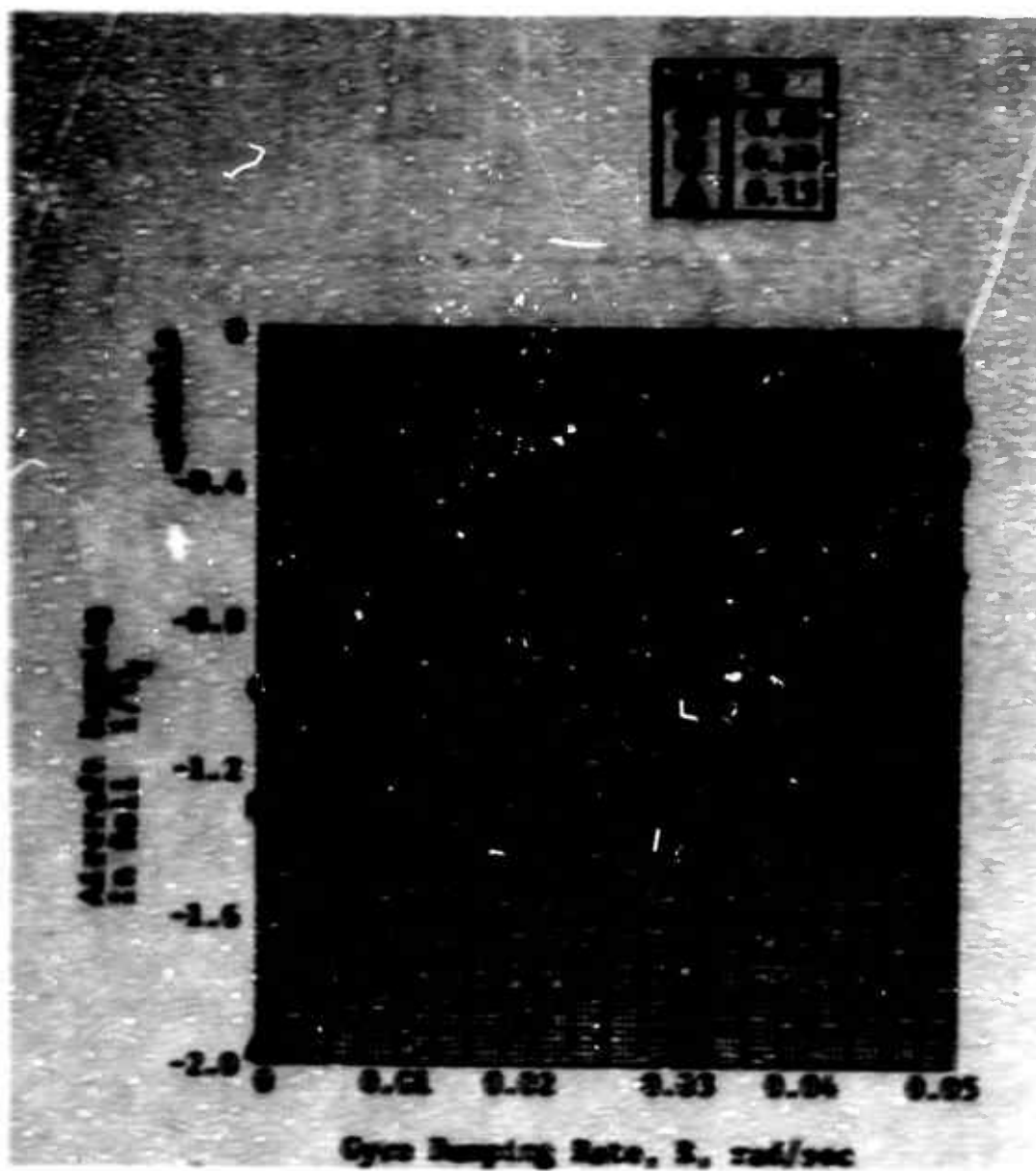


Figure 11. Effect of Synagyre Stabilizer Parameters on the lateral dynamic characteristics of the 269-A Helicopter (Hover).



**Figure 12. Effect of Gyroscopic Stabilizer Parameters on the Lateral Dynamic Characteristics of the 269-A Helicopter (15 Knots).**



**Figure 13.** Effect of Dynagyro Stabilizer Parameters on the Lateral Dynamic Characteristics of the 269-A Helicopter (70 knots).

For the periodic mode in hovering, Figure 11 also shows the variation of aircraft period of oscillation as a function of Dynagyro damping rate. For aperiodic modes in forward flight, only aircraft damping rates are presented in Figures 12 and 13.

Figures 14 through 16 show the effect of the Heading Assist Gyro damping ratio  $k_p/C_p$  on the helicopter time to half amplitude in yaw for different pilot to gyro authority ratios for the selected speed runs.

It can be seen from these figures that the aircraft damping (time to half amplitude) is a function of the NMS damping rates  $k$  and  $k_p/C_p$  and the authority ratios  $k_1$ ,  $k_2$ , and  $k_3$ . In general, for constant values of  $k$  and  $k_p/C_p$  the aircraft damping increases with increasing gyro authority ratio. Also, for constant value of  $k$  an increase in NMS damping increases aircraft damping in pitch and yaw and reduces aircraft damping in roll.

A compromise must therefore be made in the selection of the Dynagyro damping rate  $k$  such that it provides proper damping in both the pitch and roll axes of the aircraft. This is necessary since the shaping of the pitch and roll signal is made simultaneously by the selected damping rate of the Dynagyro.

Figures 17 and 18 show the variation of time constants for the aircraft longitudinal and lateral degrees of freedom, respectively, as functions of forward speed and for constant values of gyro authority ratios. The time constants  $\tau_0$  and  $\tau_1$  are defined as the time increments required to attain 63 percent of the new steady-state values of forward speed and sideslip after applying longitudinal and lateral control step inputs, respectively.

Examining the results of these figures, it can be noted that for a given forward speed an increase in gyro authority ratio results in an increase in the time constants  $\tau_0$  and  $\tau_1$ , and thus causes a reduction in aircraft response.

The analog simulation results discussed above were used for optimization of basic NMS design parameters which are presented in Table I.

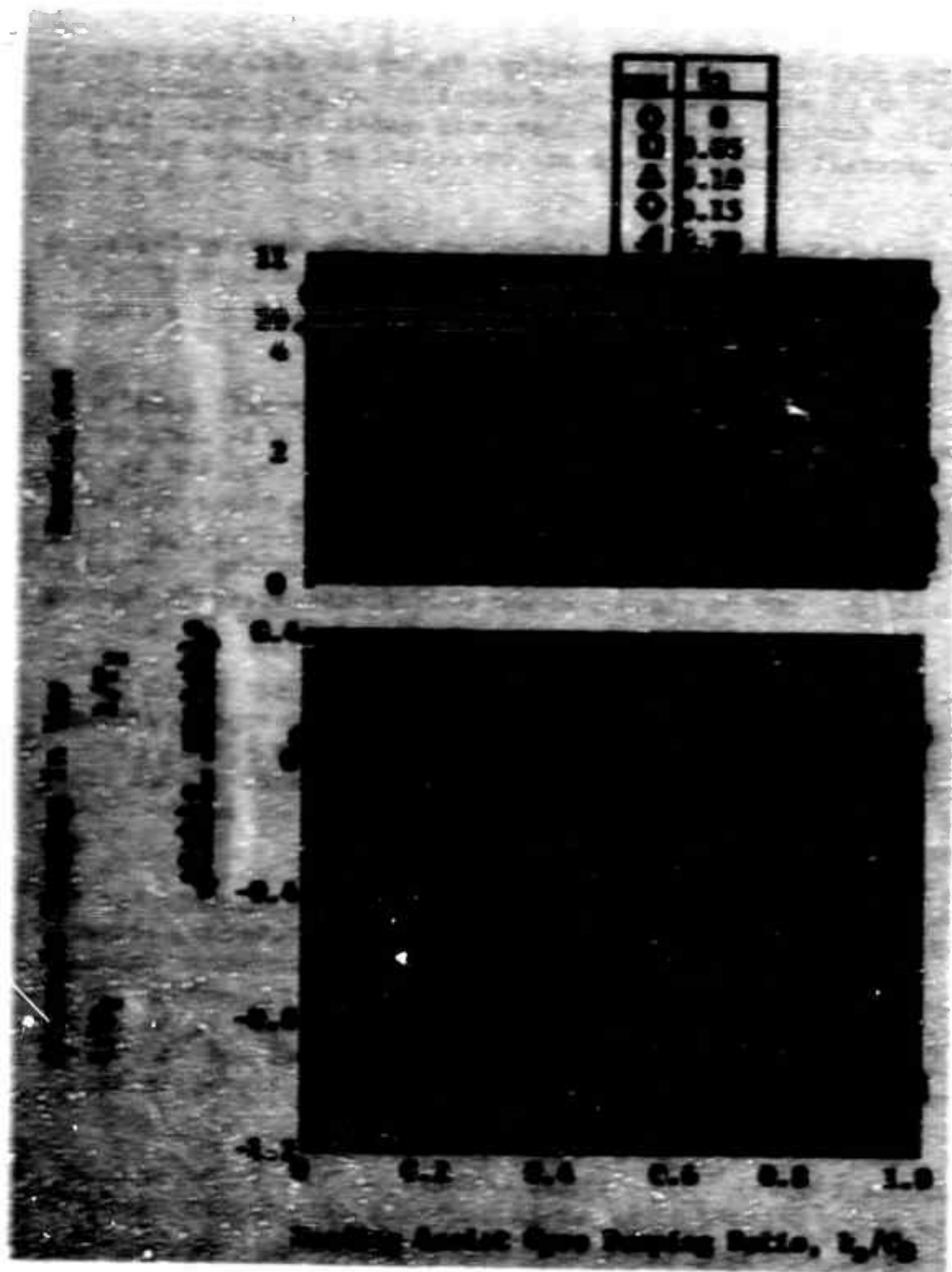


Figure 14. Effect of the Heading Assist Gyro Stabilizer Parameters on the Directional Characteristics of the 269-A Helicopter (Hover).

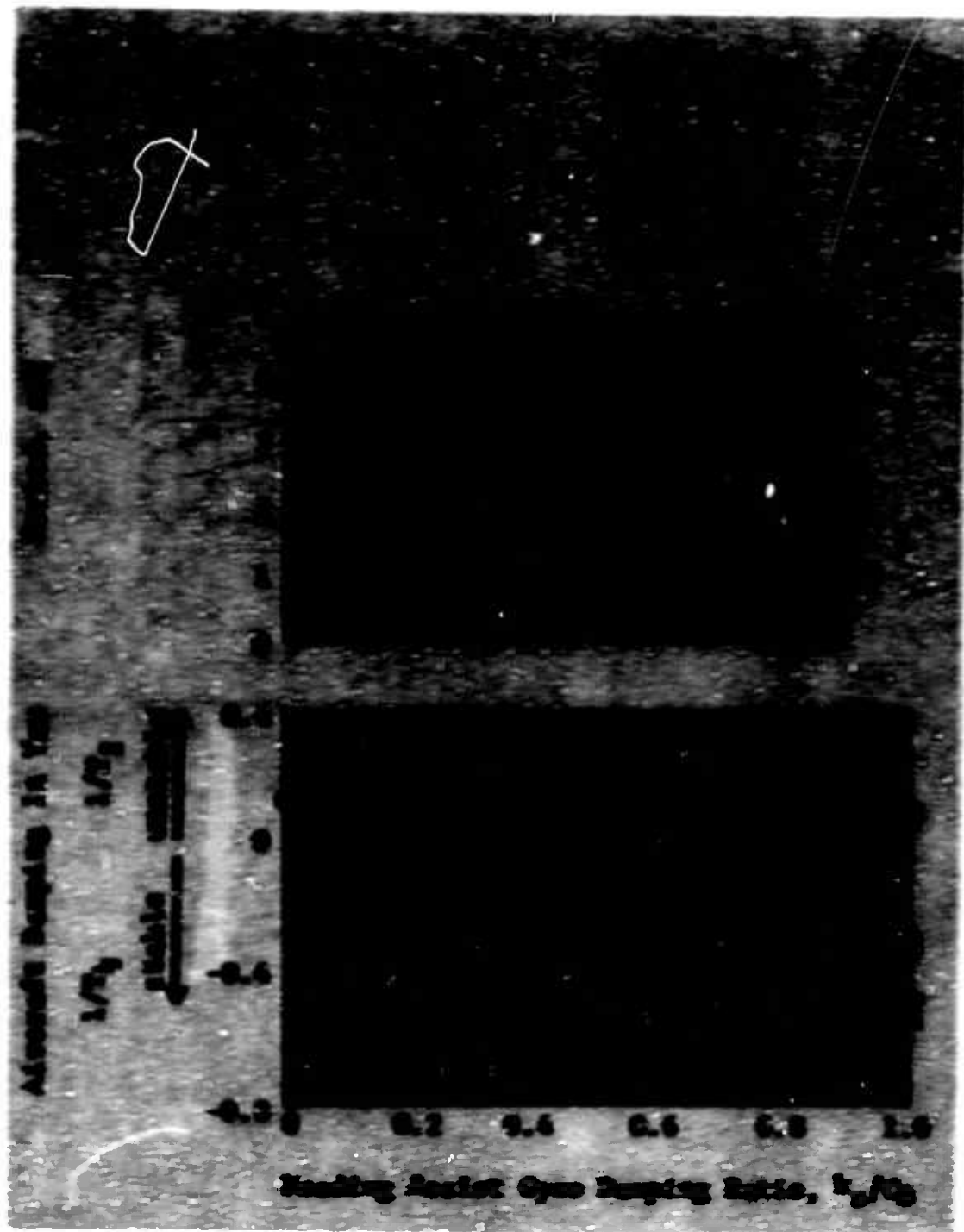
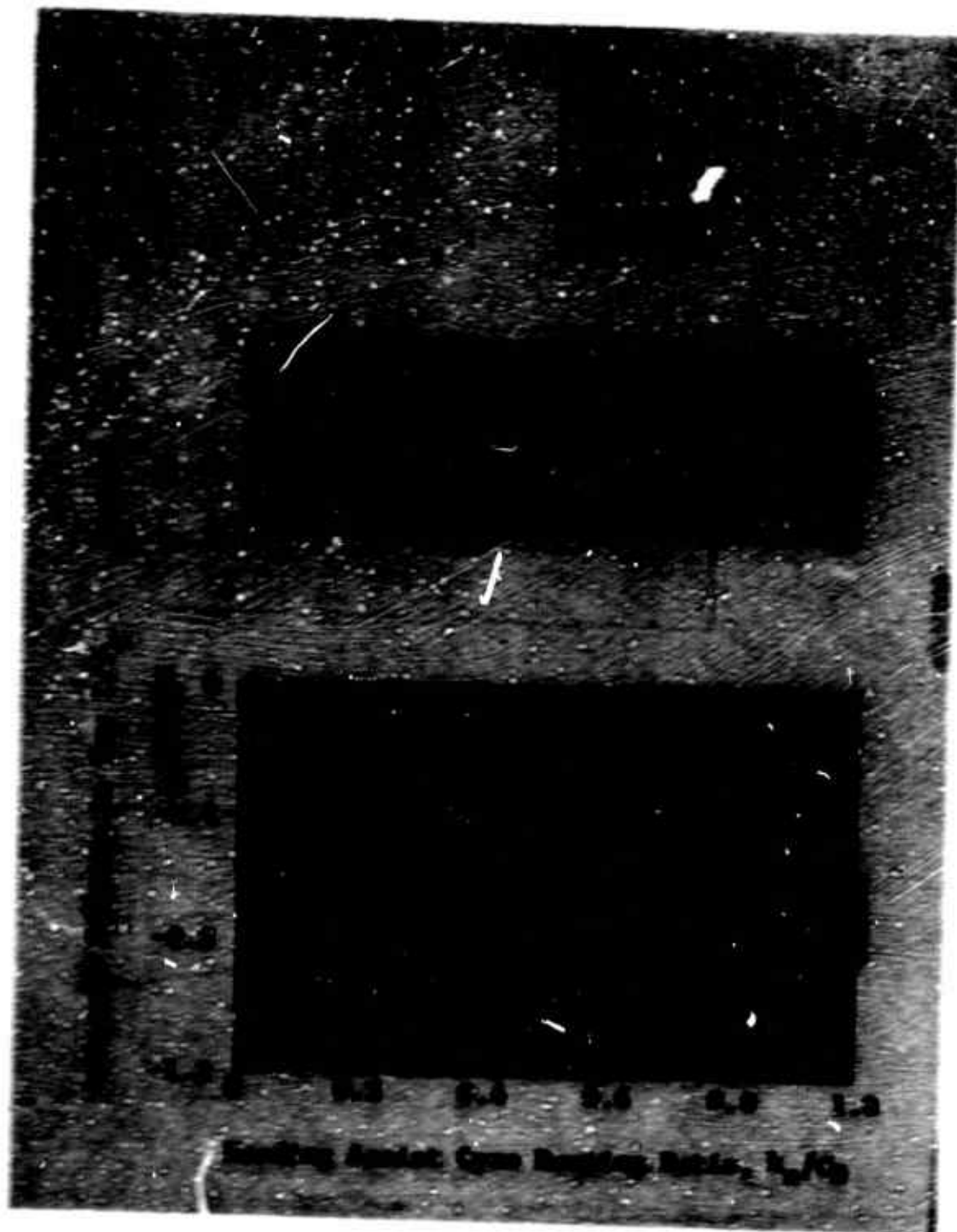


Figure 13. Effect of the Heading Assist Gyro Stabilizer Parameters on the Directional Characteristics of the 269-A Helicopter (35 Shots).



**Figure 16. Effect of the Heading Assist Gyro Stabilizer Parameters on the Directional Characteristics of the 26<sup>A</sup>-4 Helicopter (75 Knots).**



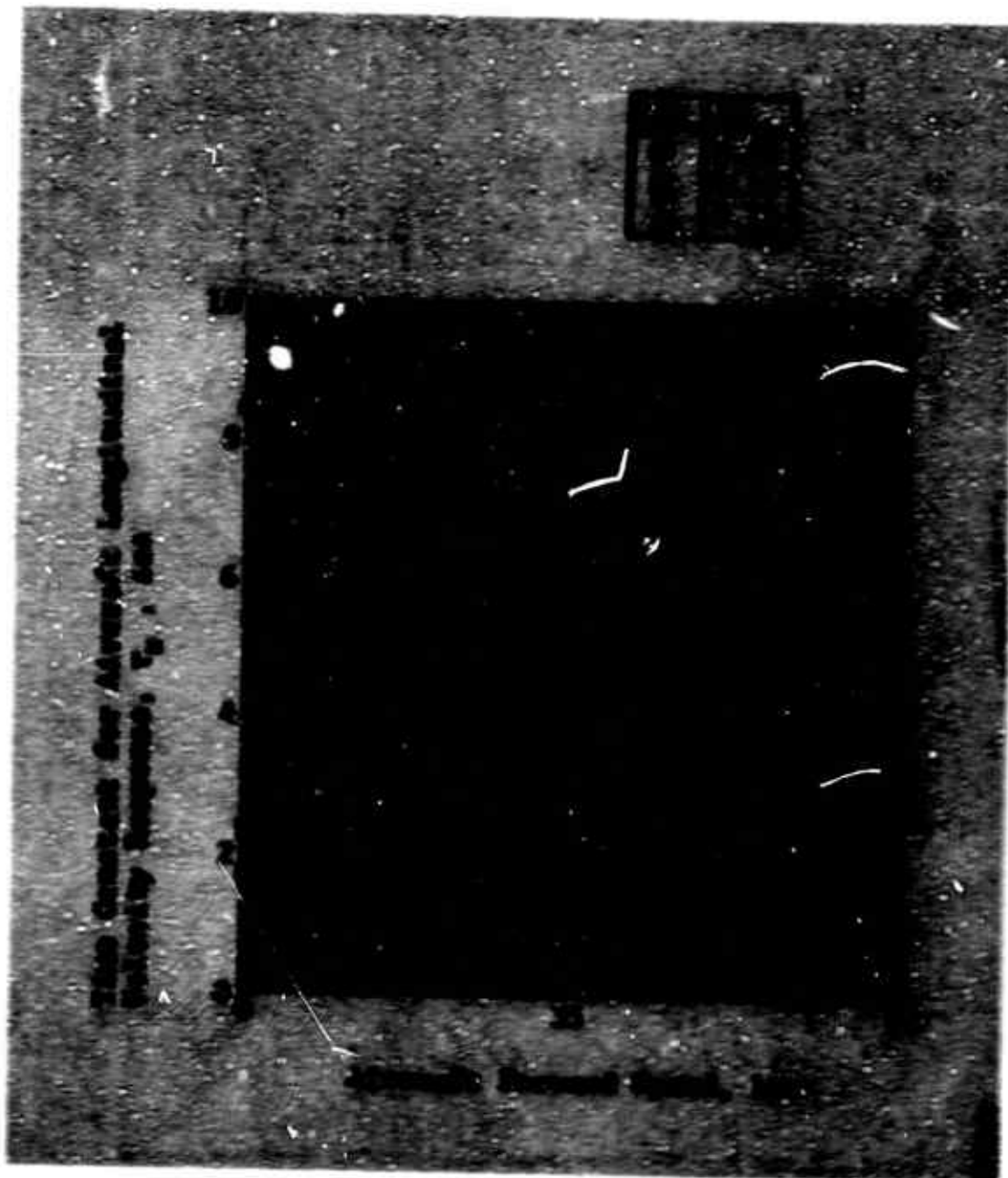
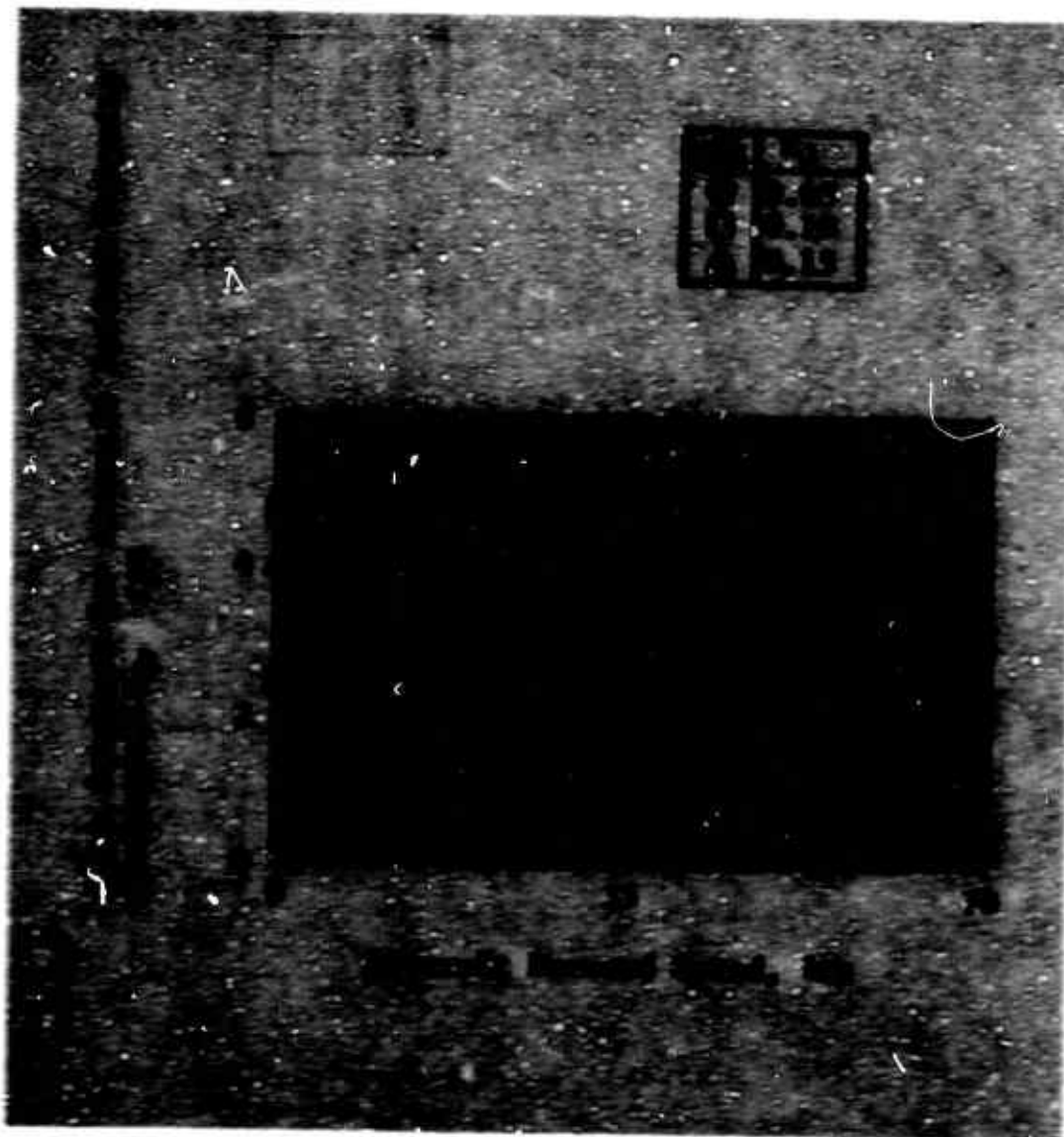


Figure 17. Time Constant for Aircraft Longitudinal Velocity Response Versus Rotor Advance Ratio for Various Pilot/Dynagyro Authority Ratios,  $R = 0.0075$ .





**Figure 18. Time Constant for Aircraft Lateral Velocity Response Versus Rotor Advance Ratio for Various Pilot/Dynagyro Authority Ratios,  $R = 0.0075$ .**

#### **IV. RELIABILITY EVALUATION OF THE MSAS**

As mentioned previously, the development cycle of the MSAS included a reliability evaluation of the system's components. For this purpose, the Dynagyro and the Heading Assist Gyro were subjected to endurance tests of 1000 and 825 hours duration, respectively, under simulated aircraft operating conditions. A description of the test program and the results obtained are presented below.

##### **A. DESCRIPTION OF THE TEST APPARATUS**

A photograph of the test apparatus used during the reliability evaluation of the MSAS is shown in Figure 19. This apparatus consisted of the following equipment and instrumentation:

##### **1. Hydraulic System**

The hydraulic system is comprised of a hydraulic supply unit, plumbing and related valving. Hydraulic power for the gyro motors and tilt table actuator was provided by a constant pressure Whithead pump, Model No. W073001A32-16, regulated to 1500 psi. The pump was driven by a 3-HP electric motor. The hydraulic system utilized a special grade oil conforming to MIL-H-5606A as the system fluid.

The hydraulic plumbing schematic is shown in Figure 20. Fluid flow to the gyro motors was controlled by a two-port on/off valve. A line check valve was connected in parallel with the flow through the motor and oriented such that when pressure to the motor was cut off, the return fluid pressure buildup due to gyro inertia would bleed through the check valve. This reduced the acceleration torque on the gyro and fluid cavitation in the motor.

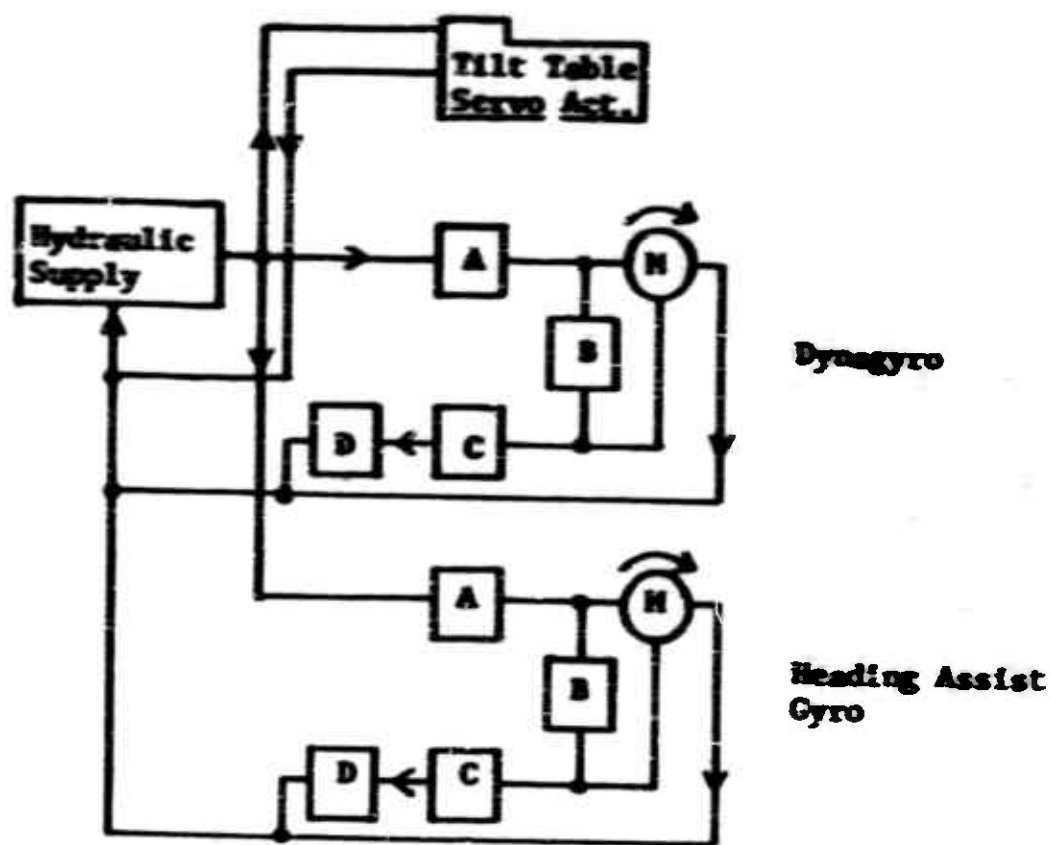
Fluid flow was regulated with a Marsh instrument needle valve located in the return line of each motor circuit, downstream from the check valve connection. The valve was adjusted to provide the desired gyro rpm.

##### **2. Tilt Table**

The tilt table provided the mounting platform for the MSAS and was used to simulate the aircraft motions about one axis. Step



**Figure 19. Test Apparatus of MSAs During Reliability Evaluation.**



<u>Item</u>	<u>Function</u>	<u>Manufacturer</u>
A	Shutoff Valve	Barksdale
B	Check Valve	Spartan
C	Flow Regulator	Marsh Instrument
D	Flow Sensor	Servo Systems
M	Hydraulic Motor	Whitehead

Figure 20. Bloc' Diagram of the MSAS Hydraulic System.

and sinusoidal motions having a maximum amplitude of  $\pm 20^\circ$  could be attained.

The table was driven by a hydraulic servo actuator whose sinusoidal motions were controlled with a function generator. Step inputs were accomplished manually.

### 3. Actuator Control Force Simulators

The actuator force simulation was achieved with spring loaded, caliper type, nylon friction pads acting against the idler bellcrank. The force exerted by these pads was a function of the spring preload. Control forces for a given test point were set by changing the preload via a threaded plunger. Table III presents the magnitudes of the control forces used during this evaluation. The control force requirements of the MSAS were based on data obtained from tests of boost actuators (Reference 1) during a previous contract.

### 4. Instrumentation

The major components of the MSAS test instrumentation consisted of a function generator, gyro output sensors, an automated control panel and an oscillograph recorder. A schematic of the instrumentation system is given in Figure 21.

#### a. Function Generator

The function generator, Hewlett Packard Model 202A, provided sinusoidal motion and varying frequency inputs through an amplifier circuit to the servo controlled actuator driving the tilt table.

#### b. Output Sensors

The gyro output sensors and their related functions are given in Table IV.

The gyro position potentiometers were mechanically coupled to the Gyro control output rods and driven by the idler bellcranks through parallel linkages. Electrical outputs from these sensors were coupled to the oscillograph through appropriate series and damping resistors.

TABLE III					
RELIABILITY EVALUATION TEST CYCLE OF MSAS					
Amplitude Frequency	Control Force Preload, Grams				
	+5°	+10°	+15°	+17.5°	Total
0.5 cps	135	163	190	204	692
1.0 cps	163	217	272	299	951



**TABLE IV**

**MS&S INSTRUMENTATION SUMMARY**

<b>Function</b>	<b>Sensor Type</b>	<b>Calibration</b>
<b><u>Dynagyro</u></b>		
Pitch position	Bourns #3585-10K Potentiometer	8.2 deg/in.
Pitch link force	Strain Gage Flexure 350-ohm Bridge	1000 gm/in.
Roll position	Bourns #3585-10K Potentiometer	8.5 deg/in.
Roll link force	Strain Gage Flexure 350-ohm Bridge	1000 gm/in.
RPM	Electric Products #3055A Magnetic Pickup	2190 rpm/in.
Hydraulic flow	Waugh #FL-65B Frequency Generator	1.143 gm/in.
<b><u>Heading Assist Gyro</u></b>		
Yaw position	Bourns #3585-10K Potentiometer	8.3 deg/in.
Yaw link force	Strain Gage Flexure 350-ohm Bridge	1500 gm /in.
RPM	Electro Products #3055 Magnetic Pickup	8760 rpm/in.
Table position	Helipot J SP-CT-RS 10K Potentiometer	10.2 deg/in.



The control force sensors were "C" section strain links connected in series with the gyro gimbal and idler bellcrank. The sensing element for each link consisted of a 350-ohm four-gage bridge whose outputs were coupled to the oscillograph through the Bridge Balance Control Unit.

The rotational speed of the gyros was measured using self-energizing Electro Products magnetic pickups, Model 3055A. Their output was monitored on the control panel meters and recorded by the oscillograph (Consolidated Electronics Model 5-114P4-18).

Hydraulic fluid flow was measured with a Waugh Model FL-6SB flow sensor which was coupled into the hydraulic return line immediately following the flow control needle valve. The flow of either gyro was selectively monitored by installing the sensor in the appropriate return line.

The tilt table position sensor was directly coupled to the pivot axis of the table. Electrical hookup was basically the same as that of the gyro position potentiometers.

c. Control Panel

The control panel contained the recording instrumentation and control system for continuous and remote recording and operation of the test apparatus. The sensor circuits contained in the control panel are the single-axis gyro position and rpm, the two-axis gyro rpm and the hydraulic flow sensor circuit. The remainder of the circuitry is related to the automatic calibration and recording, a hydraulic cutoff circuit and a running time meter.

The system calibration and test data were recorded automatically at hourly intervals for the cycling portions of the test. Step inputs were conducted manually through the use of override circuits which provided for manual operation of the oscillograph.

An automatic hydraulic cutoff circuit was provided keyed to gyro rpm, which shut off the complete system if rpm deviated  $\pm 10\%$  from the test value.

## **B. DATA ACQUISITION AND ANALYSIS**

### **1. Test Procedures**

The reliability evaluation test procedure consisted of continuous operation of the MSAS while it was subjected to varying excitation amplitudes and frequencies simulating representative aircraft motions. The endurance time accumulated by the Dynagyro and Heading Assist Gyro while operating under a variety of simulated helicopter flight conditions is summarized in Table V.

Time history traces of the MSAS due to sinusoidal excitation of the tilt table were automatically recorded at hourly intervals, while the step input excitations were applied manually on an average of three inputs per day.

Visual inspection of the system was conducted daily. In the event that a failure was suspected or apparent, the test was discontinued until the cause was determined and the corrective action incorporated. The chronological history of the test program is summarized in the Appendix.

### **2. Data Reduction**

Typical oscillograph recordings of the Dynagyro and Heading Assist Gyro response due to step and sinusoidal inputs obtained during the test program are presented in Figures 22 through 25.

The Dynagyro step response data, such as presented in Figure 22, were utilized to determine the gyro damping rate  $R$ . This parameter was obtained as a time rate of change of the gyro pitch attitude. The sinusoidal response data, such as shown in Figure 23, were used to monitor control link force, precessional coupling, and gyro and table amplitudes.

The Heading Assist Gyro step response data shown as an exponential decay curve in Figure 24 were used to obtain the damping characteristics of the gyro; i.e., the spring rate -

TABLE V					
TEST HOUR SUMMARY OF MSAS					
Table Amplitude	$\pm 5^\circ$	$\pm 10^\circ$	$\pm 15^\circ$	$\pm 17.5^\circ$	
Frequency (cps)	<u>Dynagyro</u>				
	Hours	Hours	Hours	Hours	Total Hours
0.5	225	200	50	25	500
1.0	225	200	50	25	500
Frequency (cps)	<u>Heading Assist Gyro</u>				
	Hours	Hours	Hours	Hours	Total Hours
	Hours	Hours	Hours	Hours	Total Hours
0.5	225	200	50	25	500
1.0	225	100			325

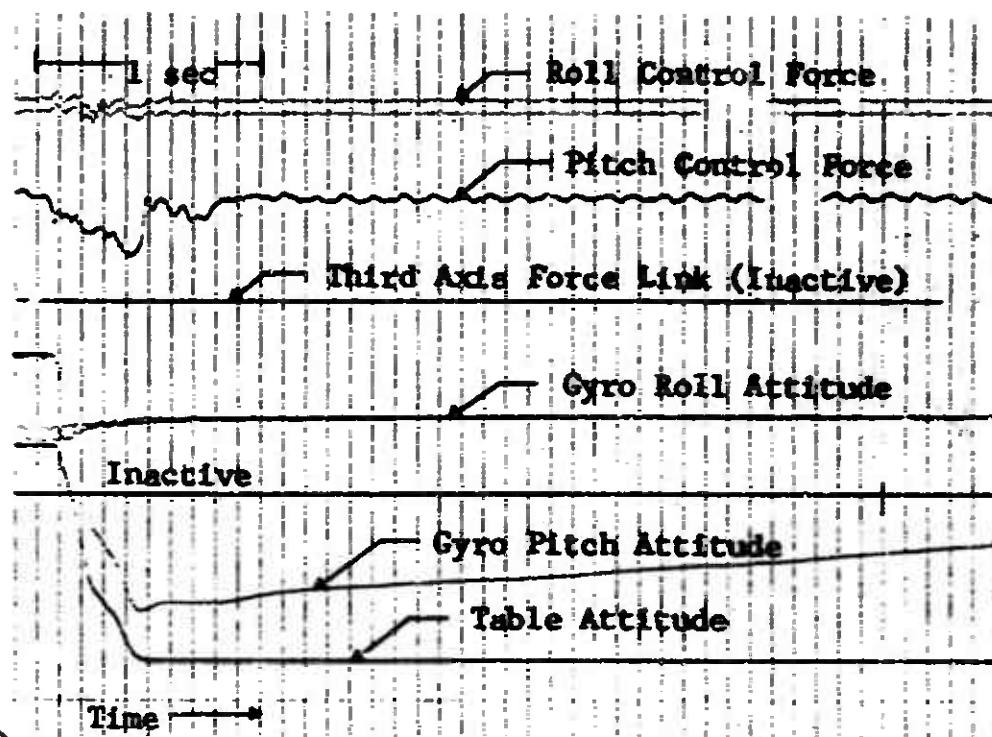


Figure 22. Time History Response of the Dynagyro to a Step Input.

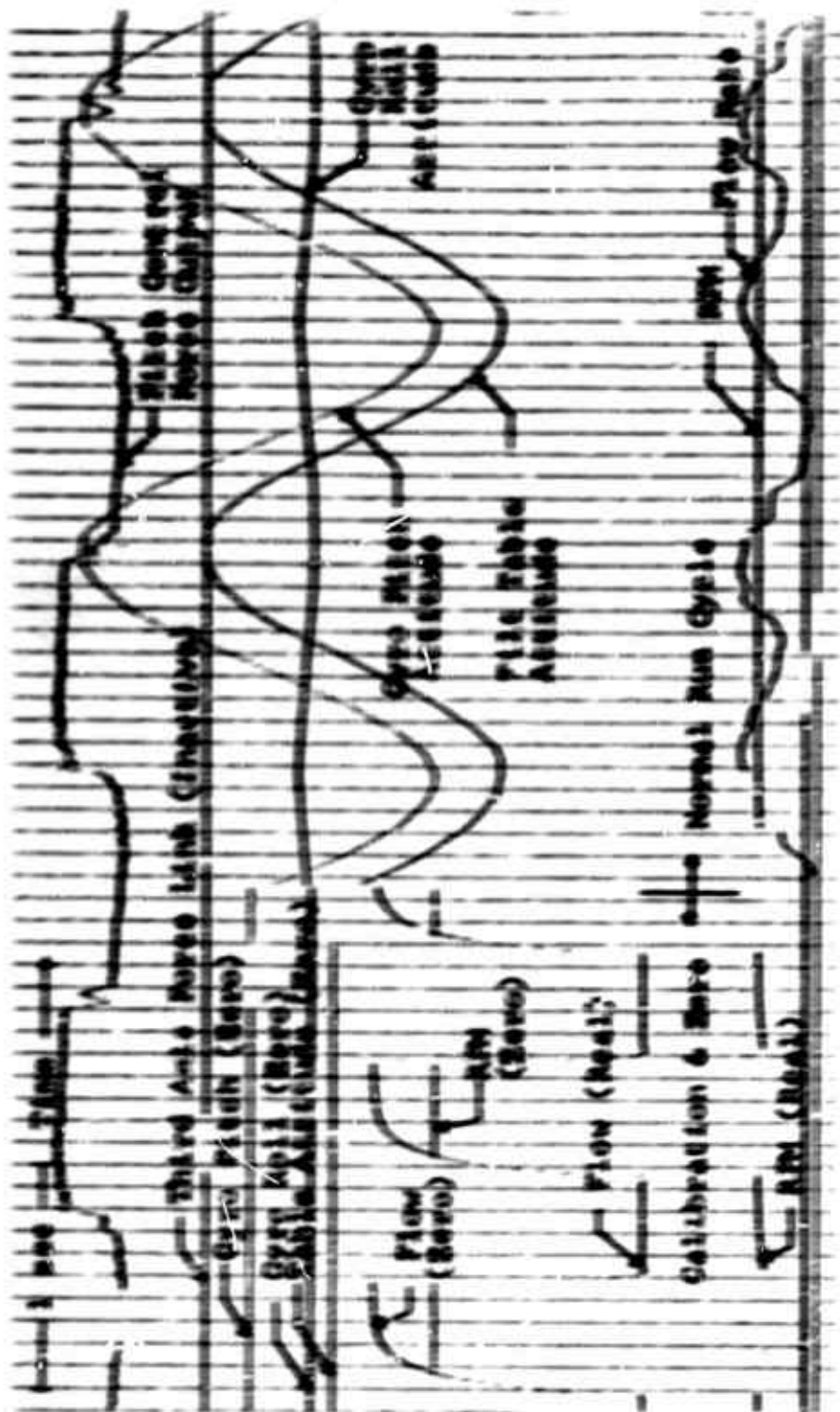
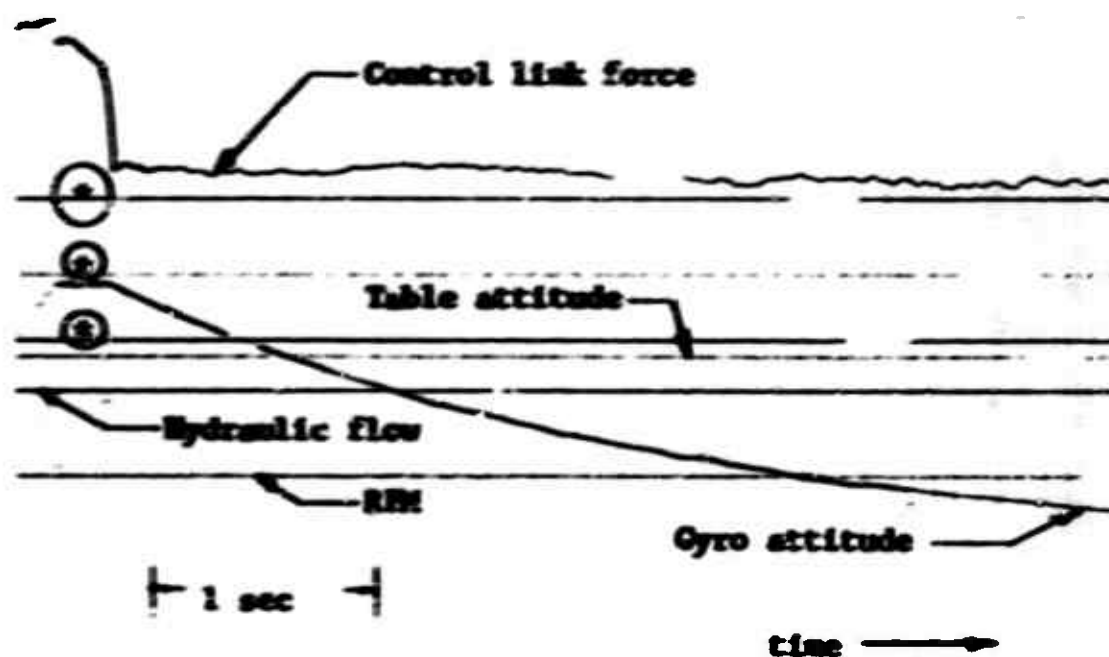
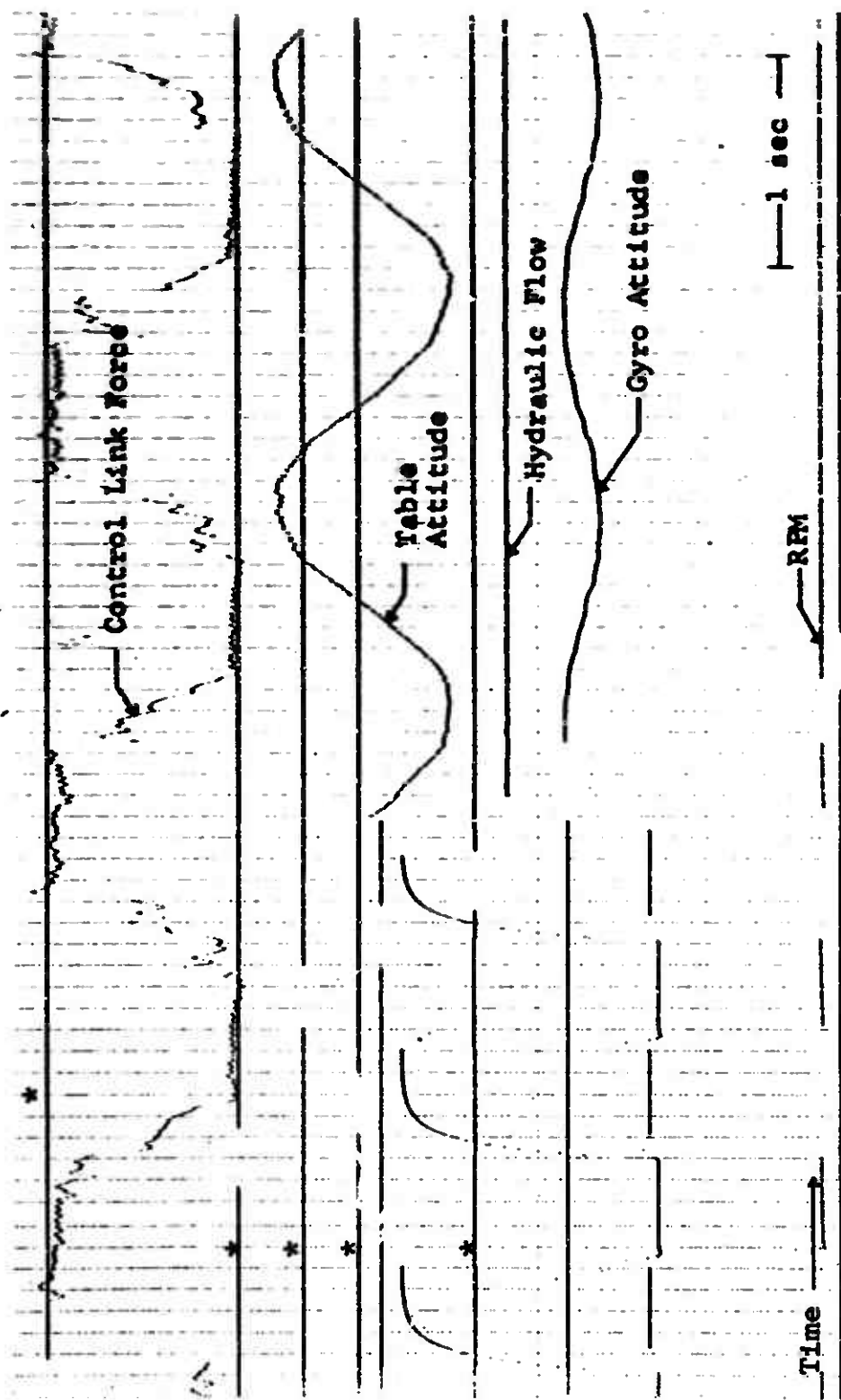


Figure 23. Time History Response of the Dynagyro to Sinusoidal Input.



\* 2 Axis Gyro (Inactive Channels)

Figure 24. Time History Response of the Heading Assist Gyro to a Step Input.



\* 2 Axis Gyro (Inactive Channels)

Figure 25. Time History Response of the Heading Assist Gyro to a Sinusoidal Input.

specific damping ratio,  $k_s/C_D$ . The sinusoidal response data (Figure 25) were used to monitor control link force, gyro and table attitude as well as phase angle between the gyro and the tilt table attitudes.

### C. TEST RESULTS

This section presents a summary of the measured operational characteristics of the MSAS together with a discussion of the system's reliability. The most important operational characteristics of the MSAS are the damping rate and precessional coupling of the Dynagyro, and the damping rate and phase angle of the Heading Assist Gyro.

#### 1. Dynagyro

The time history data obtained during the reliability tests were analyzed to obtain Dynagyro damping rates and precession coupling due to simulated control force inputs.

The measured damping rate data are summarized in Figure 26 as a function of running hours accumulated. A distinction is made in the data presentation between the types of tilt table input conditions for which the datum points were obtained. During the 1000 hours of tests, the damping rate averages 0.0085 rad/sec, with maximum variation of +14%. Based upon the analog computer results, this satisfies the requirement of the system.

Gyroscopic coupling data for simulated control inputs applied to the gyro are presented in Figure 27 as a function of running hours accumulated. The coupling observed was approximately 4% at 0.5 cycle per second table excitation frequency. At 1.0 cycle per second, the precession is reduced to approximately 2%. The reason for this can be seen by examining the expression defining the maximum gyro precession for a sinusoidal excitation:

$$\left(\frac{\delta}{\beta}\right)_{\max} = \frac{(T_{YA})_{\max}}{I_s \Omega \omega_y \beta_{\max}} \quad (10)$$



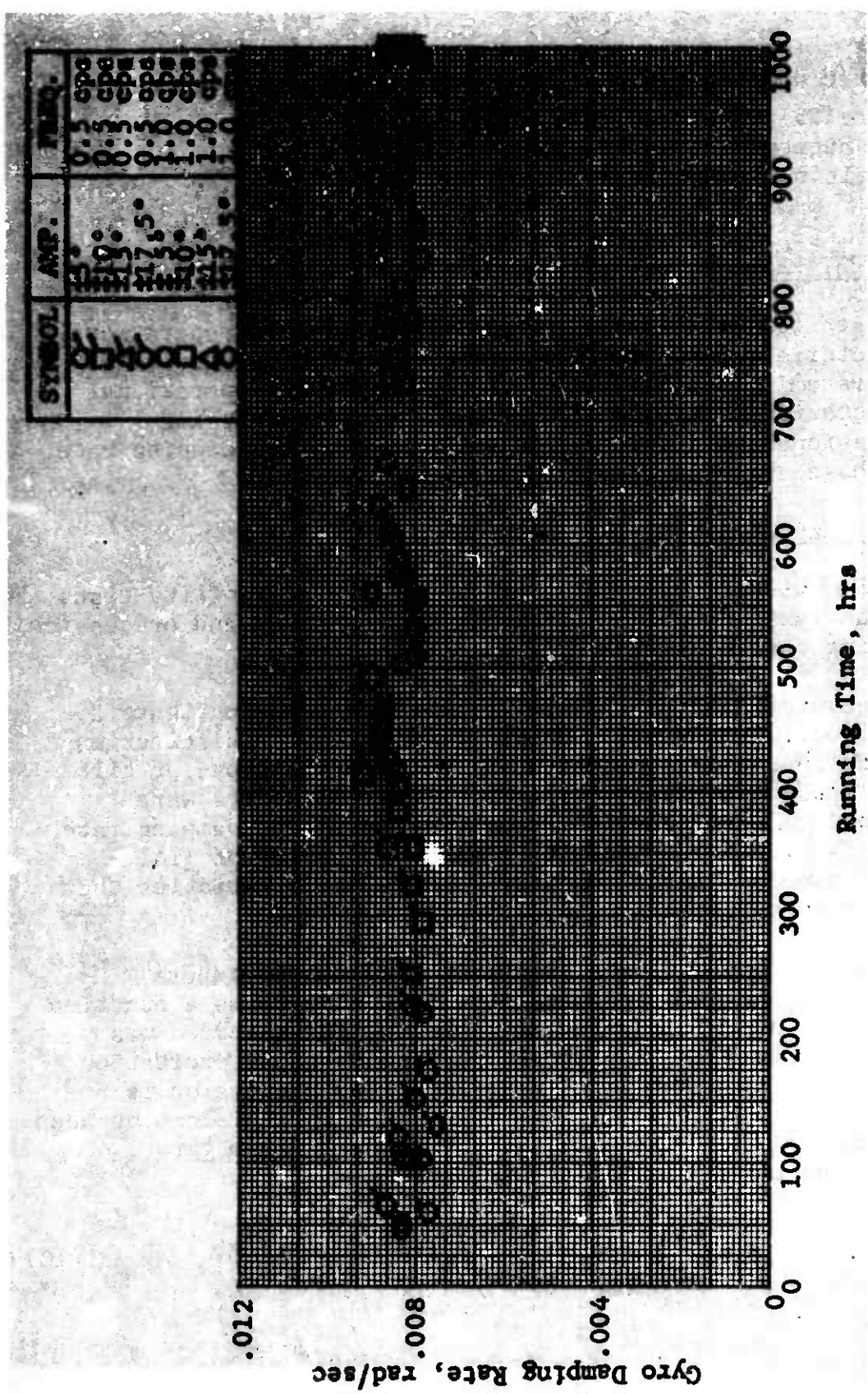


Figure 26. Dynagyro Damping Rate History Versus Cumulative Test Hours.



From equation (10), the coupling ratio  $\delta/\beta$  is seen to be inversely proportional to the input frequency ( $\omega_y$ ). Although the applied control force  $(T_{YA})_{\max}$  is increasing with ( $\omega_y$ ) (Table III), its rate of increase is less than the increase in excitation frequency. Consequently, an overall decrease in gyroscopic coupling occurs with increased excitation frequency. The amount of coupling obtained during these tests correlates with the average design value selected, 5%.

All other variables monitored during the Dynagyro Reliability tests were reviewed for consistency and repeatability. These variables, which include gyro rpm, hydraulic flow rate and control force, remained unchanged during the tests.

## 2. Heading Assist Gyro

The damping rate for the Heading Assist Gyro is defined as the ratio of spring rate  $k_s$  to specific damping coefficient  $C_D$ . This ratio can be obtained analytically by solving the rate gyro equation of motion, equation (9), for  $q = \eta P(t)$ , where  $P(t)$  is unit pulse function at  $t = 0$ . The resulting equation is

$$\frac{\eta}{\eta_0} = e^{-\left(\frac{k_s}{C_D}\right)t} \quad (11)$$

where  $\eta$  is the time varying gyro attitude and  $\eta_0$  is the initial displacement of gyro attitude.

Experimentally, time histories of step inputs obtained during the reliability evaluation of the Heading Assist Gyro were processed to obtain the slope of the exponential decay of the gyro attitude. When plotted on semilogarithmic coordinates, this slope is the damping ratio  $k_s/C_D$ . Test results obtained are summarized in Figure 28 as a function of running hours accumulated. From this figure, it can be seen that the damping rate average is 0.33, with variations of  $\pm 7\%$  over the total test hours accumulated.

SYMBOL	AMP.	FREQ.
○	±5°	0.5 cps
□	±10°	0.5 cps
△	±15°	0.5 cps
○	±17.5°	0.5 cps
○	±5°	1.0 cps
□	±10°	1.0 cps

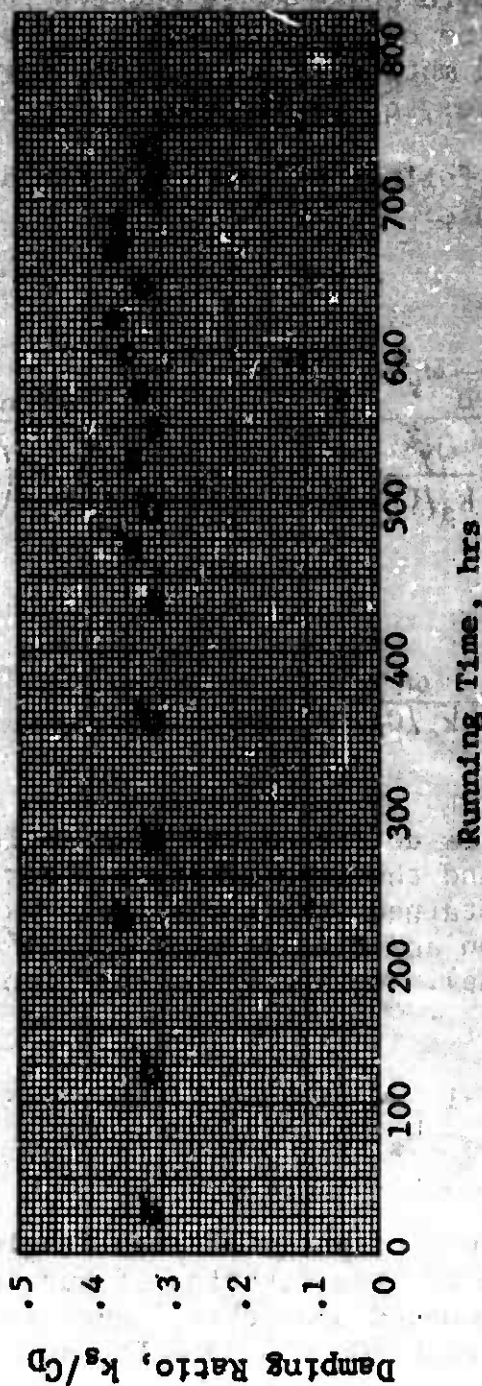


Figure 28. Heading Assist Gyro Damping Ratio Versus Cumulative Test Hours.

The Heading Assist Gyro phase angle between input rate and output position can be obtained analytically by solving the gyro equation of motion, equation (9), for a sinusoidal forcing function (i.e.,  $q = A \sin \omega t$ ).

This results in the following function after describing the gyro attitude response:

$$\eta = \frac{A}{(k_s/C_D) \omega_y} \left\{ \frac{\frac{1}{k_s/C_D} \omega_y^2}{1 + \frac{\omega_y^2}{k_s/C_D}} e^{-(k_s/C_D)t} + \frac{\omega \sin(\omega t - \psi_r)}{\left\{ 1 + \left( \frac{\omega}{k_s/C_D} \right)^2 \right\}^{\frac{1}{2}}} \right\} \quad (12)$$

where

$$\psi_r = \tan^{-1} \frac{\omega}{k_s/C_D} \quad (13)$$

The phase angle  $\psi_r$  is defined as the lag angle between the input angular rate and the gyro attitude. For the actual time history data obtained, the phase angle is the time lag between gyro position and the integral of the angular rate input (table attitude). As such, the position phase angle  $\psi_p$  becomes

$$\psi_p = \tan^{-1} \frac{\omega}{k_s/C_D} - 90^\circ \quad (14)$$

The experimental values of position phase angle obtained are summarized in Figure 29 as a function of running hours accumulated. Superimposed upon this figure is the theoretical curve for  $\psi_p$  based on  $k_s/C_D = 0.33$ . It can be seen from these results that the phase angle measured varies within  $\pm 3^\circ$  due to experimental errors believed to be due primarily to higher harmonics generated by the tilt table.

SYMBOL	AMP.	FREQ.
○	±5°	0.5cps
□	±10°	0.5cps
△	±15°	0.5cps
○	±17.5°	0.5cps
○	±5°	1.0cps
□	±10°	1.0cps

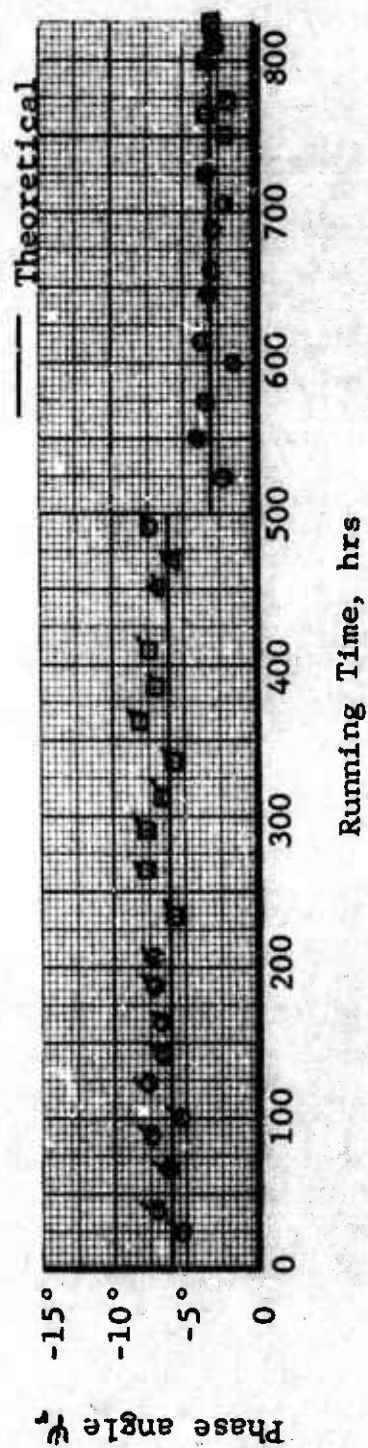


Figure 29. Heading Assist Gyro Phase Angle Versus Cumulative Test Hours.



Position phase angle as shown in Figure 29 is negative, which in this case indicates that the gyro attitude leads the table attitude.

#### D. MECHANICAL EVALUATION OF THE MSAS

The MSAS was subjected to a 1000-hour operational test using simulated aircraft motion inputs to evaluate system maintainability, reliability and life expectancy. A chronological history of the system performance obtained is given in the Appendix. Problem areas encountered and corrective action taken during this evaluation are summarized below.

##### 1. Operational Problems and Solutions

###### a. Dynagyro

The only major operational problem encountered during the mechanical evaluation of the Dynagyro was related to the damper rod and track assembly.

During early operation of the Dynagyro, the damper rods rotated in their mounting pivots. This was attributed to two factors; namely, rotation due to windage and rotation during static handling. The problem was corrected by modifying the damper rod design, which incorporated stops, limiting rotation to approximately  $\pm 10^\circ$ . This corrective action, performed after approximately 350 hours of tests, successfully eliminated the problem.

The Oilite tracks, after 400 hours of operation, lost their lubricating property, thereby leading to rapid damper rod wear. This was attributed to the burnishing of the Oilite contact surface and closing up the oil bearing pores of the material. The condition was corrected by changing damper track material from bronze to iron, and by doubling the contact surface area. After this modification, no further damper wear problems were encountered and the system operated successfully through the balance of the tests.

Minor problem areas encountered during the tests were with the Waterman flow regulator, Model 320-2-1.7, and with fretting corrosion of the motor drive shaft spline. The flow regulator did not operate satisfactorily above 3000 rpm. As a corrective measure, a needle-type regulator valve was used for replacement. Fretting corrosion was noted on the drive shaft spline during the 500-hour inspection. This was attributed to improper lubrication at initial assembly. The application of molybdenum disulfide base lubricant eliminated any additional wear.

b. Heading Assist Gyro

The operational problems encountered with the Heading Assist Gyro were related to the transmission assembly seals and the pivot axis assembly.

The transmission assembly lip seals exhibited severe leakage after 264 hours of operation. These seals were replaced and the oil was replenished. After an additional 16 hours of operation, the seal leakage reappeared along with an increase in transmission temperature up to 250°F. This oil leakage and transmission overheating problem was attributed to the improper selection of the oil seal for this application. As a corrective measure, the transmission lip seals were replaced with the felt seals and the transmission oil lubricant was changed to a medium weight, high temperature silicone grease. The combination of felt seals and grease lubricant operated satisfactorily at a reduced transmission temperature of about 110°F throughout the remaining part of the test program.

Another operational problem which occurred after 757 hours of operation was a significant increase in noise level of the Heading Assist Gyro. The assembly was shut down, disassembled and visually inspected (see the inspection report included in the Appendix). After careful examination of the assembly, an excessive play was noted in the pivot axis bearings in axial and radial directions.



This condition was attributed to an axial line-to-line /in in the clamp-up of the bearings instead of to preloading the assembly. This play was aggravated by the tilt table excitation, which due to servo-valve malfunction was more square than sinusoidal during the later stages of the test program. Temporary corrective measures were taken at this time to repair the gyro without correcting the table. However, continuous operations with these table excitations were considered to be detrimental to the gyro operation; consequently, the tests were terminated after 825 hours of accumulated endurance time.

## 2. Maintainability

The required operational maintenance of the M&S during the evaluation testing was minimal, consisting of visual inspections only. Lubrication of the Dynagyro assembly was not required since all bearings were of the sealed type. The Heading Assist Gyro lubrication requirements were limited to packing the transmission gears and appropriate bearings with silicone grease on assembly; all other bearings were of the sealed type. The universal joints for both assemblies were prelubricated by the manufacturer.

The hydraulic motors used during the tests performed satisfactorily throughout the program and required no servicing.

Based on the results of the operational evaluation tests, the following maintenance procedures are recommended:

**M&S 15-hour-interval visual inspection.**

### Item

All Bearings	axial Clearance
Damper Assembly	Rot Wear
Ball Retaining Nut	Torque - Dynagyro, 12-15 in-lb; Heading Assist Gyro, 30-40 in-lb

**MSAS Service:**

Lubricate transmission assembly - 500 hours  
Replace damper rod assembly - 1000 hours

**3. System Reliability and Life Expectancy**

Based on operational test results of the MSAS components, and with the corrective actions taken, the system reliability is expected to be in excess of 1000 hours. It is believed that the MSAS, if properly maintained, will operate successfully well in excess of 1000 hours.

## **V. CONCLUSIONS AND RECOMMENDATIONS**

Based on the results of this study, the following conclusions and recommendations are made:

1. Analog computer analyses show that the use of a three-axis mechanical stability augmentation system which is compact, lightweight, and installable within the aircraft will provide typical helicopters with stability characteristics which meet existing handling qualities criteria.
2. The 1000-hour reliability test program has demonstrated structural integrity and functional feasibility of a three-axis mechanical stability augmentation system (MSAS) consisting of the Dynagyro and the Heading Assist Gyro.
3. The test data obtained from the program indicate that the damping characteristics of the Dynagyro and the Heading Assist Gyro are well within the optimum design limits determined from the analog computer study.
4. The MSAS developed under this program is very easy to maintain. The system's maintenance requirements consist of external inspections every 25 hours, system lubrication every 500 hours and damper assembly replacement every 1000 hours.
5. In view of the promising results obtained from this study, it is recommended that a flight test evaluation of the MSAS be conducted to establish airworthiness of the three-axis mechanical stability augmentation system for helicopters.

## VI. REFERENCES

1. George, M., Kisielowski, E., Perlmutter, A. A., "Dynagyro - A Mechanical Stability Augmentation System for Helicopters", USAAVLABS Technical Report 67-10, U.S. Army Aviation Materiel Laboratories, Fort Eustis, Virginia, March 1967.
2. Kisielowski, E., Perlmutter, A. A., Tang, J., "Stability and Control Handbook for Helicopters", USAAVLABS Technical Report 67-63, U.S. Army Aviation Materiel Laboratories, Fort Eustis, Virginia, August 1967.

## **APPENDIX**

### **CHRONOLOGICAL HISTORY, MSAS TEST PROGRAM**

This Appendix contains the chronological events of the 1000-hour reliability evaluation of the MSAS. The cumulative hours reported were from 0 to 1000 for the Dynagyro and 1000 to 1825 for the Heading Assist Gyro. The duration of the test program was 7.5 months, 3 months for the Dynagyro and 4.5 months for the Heading Assist Gyro.

A summary of the test hours and events which occurred during the test program, including operational problems, corrective actions taken and system's inspection report, are presented on the following pages.

A. OPERATIONAL PROBLEMS AND CORRECTIVE ACTIONS

1. Dynagyro

<u>Date</u>	<u>Test Hour</u>	<u>Remarks</u>
3/8/68	0	Beginning of the 1000-hour reliability tests. Visual inspection conducted after 5 minutes of operation. No. 3 damper exhibiting scratches on side face - considered noncritical. System did not attain design rpm due to hydraulic surging. Problem identified with flow regulator. Needle valve substituted.
3/14/68	51.0	Visual inspection. Damper rod No. 1 found to be reversed on track, i.e., curvature toward spin axis. No. 3 damper assembly removed and weighed for future reference. Weights: Track, 8.152 gms; damper, 10.688 gms. Cause: Incorrectly installed. Corrective Action: Reinstalled correctly.
3/20/68	125.0	Visual inspection. The following items were checked and were considered satisfactory: motor bearings drag, noise, universal backlash, gimbal bearings, spin bearings, damper assemblies. Damper rod side wear had not increased appreciably. Track surfaces not burnished. No. 3 track weight, 8.138 gms; No. 2 track weight, 7.838 gms. A cycling noise was noted during test operation. Visual inspection did not reveal any malfunction in the components. Gyro was operated without the damper assemblies; however, noise was still noted. Cause: Investigation of gyro rpm with a strobe light showed the gyro rpm to pulsate with table oscillations. Noise due to flow change through table actuator. Corrective Action: Not considered necessary. Test reinstated.

<u>Date</u>	<u>Test Hour</u>	<u>Remarks</u>												
3/25/68	226.0	Frequency 0.5 cps, amplitude $\pm 10^\circ$ . Damper assembly weights recorded:												
		<table border="1"> <thead> <tr> <th><u>No.</u></th> <th><u>Rod, gms</u></th> <th><u>Track, gms</u></th> </tr> </thead> <tbody> <tr> <td>1</td> <td>10.6130</td> <td>8.2766</td> </tr> <tr> <td>2</td> <td>10.6411</td> <td>7.8373</td> </tr> <tr> <td>3</td> <td>10.6930</td> <td>8.1305</td> </tr> </tbody> </table>	<u>No.</u>	<u>Rod, gms</u>	<u>Track, gms</u>	1	10.6130	8.2766	2	10.6411	7.8373	3	10.6930	8.1305
<u>No.</u>	<u>Rod, gms</u>	<u>Track, gms</u>												
1	10.6130	8.2766												
2	10.6411	7.8373												
3	10.6930	8.1305												
3/30/68	320	<p>Visual inspection conducted. No. 2 damper rod was found to be destroyed. Damper rods 1 and 3 were found to be in satisfactory condition.</p> <p>Cause: Detailed investigation showed dampers rotating due to air drag, hence having line contact with track. Also, dampers became loose in pivot bearings due to 'Penacolite' not adhering to bearings.</p> <p>Corrective Action: Additional weights were added to damper arms to pull their cg out-board of rubbing surface. A droplet of 'Penacolite' was added to bottom end of damper rod to prevent its pulling through bearing.</p>												
4/5/68	343.2	Oscillograph lamp failed.												
4/5/68	346.5	<p>Damper No. 1 found to be rotated <math>90^\circ</math>. Test was terminated.</p> <p>Cause: Considered same as previous.</p> <p>Corrective Action: Added additional weight to damper tips.</p>												
4/5/68	349.1	<p>Damper turned again.</p> <p>Cause: Same as above.</p>												

Date            Test  
Hour

Remarks

Corrective Action: Stops were designed and installed to prevent damper rotation.

Damper No.            Rod Assembly Weights, gms

1	11.010
2	11.041
3	11.068

4/8/68      349.1      Tests resumed.

4/10/68      396.3      Visual inspection was conducted. Damping rates were too high. Damper rods No. 1 and No. 2 showed excessive wear. Rod No. 3 had no noticeable wear. Rod and track weights were determined.

Damper No.            Rod, gms            Track, gms

1	10.973	8.225
2	11.020	7.767
3	11.065	8.058

Cause: Evaluation of problem showed that Oilite pores were closed, thereby restricting flow of lubricant and thus causing the high damping and wear rates. Also, edge wear marks on damper tracks indicated vertical misalignment of the sliding surfaces due to fabrication tolerances.

Corrective Action: Bearing surface area of damper track was doubled to prevent edge wear. Damper track material was changed from standard to super Oilite, which had the same porosity content but was made of sintered iron rather than bronze.

4/18/68      396.3      Resume tests with new damper rods and tracks.



<u>Date</u>	<u>Test Hour</u>	<u>Remarks</u>												
		<table border="1"> <thead> <tr> <th><u>Rod No.</u></th> <th><u>Rod Weight, gms</u></th> <th><u>Track Weight, gms</u></th> </tr> </thead> <tbody> <tr> <td>1</td> <td>11.037</td> <td>14.595</td> </tr> <tr> <td>2</td> <td>11.004</td> <td>13.784</td> </tr> <tr> <td>3</td> <td>10.977</td> <td>14.297</td> </tr> </tbody> </table>	<u>Rod No.</u>	<u>Rod Weight, gms</u>	<u>Track Weight, gms</u>	1	11.037	14.595	2	11.004	13.784	3	10.977	14.297
<u>Rod No.</u>	<u>Rod Weight, gms</u>	<u>Track Weight, gms</u>												
1	11.037	14.595												
2	11.004	13.784												
3	10.977	14.297												
		Tilt table did not function properly. Function generator problem was corrected, and test resumed.												
4/19/68	402.8	Visual inspection conducted. Dampers functioning properly. Frequency 0.5 cps, amplitude $\pm 15^\circ$ .												
4/22/68	420	Frequency 0.5 cps, amplitude $\pm 17.5^\circ$ .												
4/25/68	475	Frequency 1.0 cps, amplitude $\pm 5^\circ$ .												
4/25/68	498	Frequency 1.0 cps, amplitude $\pm 5^\circ$ .												
4/26/68	507	High damping rate observed visually. Test shut down. Damper rod No. 3 showed excessive wear. Weight, 10.828 gms.												

Cause: High wear rate attributed to too coarse finish of Oilite tracks.

Corrective Action: Oilite bearing faces machined to 16 rms finish. New weights:

<u>Rod No.</u>	<u>Damper Rod, gms</u>	<u>Track, gms</u>
1	11.023	14.208
2	11.998	13.385
3	11.065	13.880

The shaft driven by the hydraulic motor exhibited spline wear due to fretting corrosion; i.e., it appeared to have been heavily coated with oxide powder. The

<u>Date</u>	<u>Test Hour</u>	<u>Remarks</u>												
		<p>splines were cleaned and the angular play measured. This was found to be 0.0392 radian. The maximum play when new was 0.016 radian. This represents a wear rate of <math>23.2 \times 10^{-6}</math> radians per hour based on a linear assumption. This type of wear is attributed to the high frequency pulsations of the hydraulic motor and the lack of replenishment of lubrication.</p> <p>Corrective Action: Used a spline lubricating grease containing molybdenum disulphide, <math>MoS_2</math>.</p>												
5/1/68	507	<p>Tests resumed. Pitch force link failed.</p> <p>Cause: Broken connection.</p> <p>Corrective Action: Resoldered.</p>												
5/3/68	558.3	Table servo actuator malfunctioned. Refused to respond to input. Servo valve replaced. Tests resumed.												
5/8/68	607	Oscillograph lamp failed.												
5/15/68	731.1	Frequency 1.0 cps, amplitude $\pm 10^\circ$ . Damper assemblies weighed.												
		<table> <tr> <th><u>Rod No.</u></th><th><u>Rod, gms</u></th><th><u>Track, gms</u></th></tr> <tr> <td>1</td><td>11.0244</td><td>14.1792</td></tr> <tr> <td>2</td><td>10.9978</td><td>13.3356</td></tr> <tr> <td>3</td><td>11.0643</td><td>13.8340</td></tr> </table>	<u>Rod No.</u>	<u>Rod, gms</u>	<u>Track, gms</u>	1	11.0244	14.1792	2	10.9978	13.3356	3	11.0643	13.8340
<u>Rod No.</u>	<u>Rod, gms</u>	<u>Track, gms</u>												
1	11.0244	14.1792												
2	10.9978	13.3356												
3	11.0643	13.8340												
5/17/68	780.6	Pitch force link failure not repaired.												
5/29/68	928.8	Frequency 1.0 cps, amplitude $\pm 15^\circ$ .												
6/2/68	974.8	Frequency 1.0 cps, amplitude $\pm 15^\circ$ .												
6/3/68	1000	Test concluded.												

## 2. Heading Assist Gyro

<u>Date</u>	<u>Test Hour</u>	<u>Remarks</u>
6/8/68	1000	Amplitude $\pm 5^\circ$ , frequency 0.5 cps. Initiated testing. Seal leakage occurred after 5 hours of operation. Test discontinued. Running temperature 225°F. Manufacturer contacted.  Cause: Seal compound not suitable for high temperature operation.  Corrective Action: New seal compound 'Viton' was recommended for continuous operation at high temperature. New seals ordered.
8/6/68	1005	Amplitude $\pm 5^\circ$ , frequency 0.5 cps. Resumed testing with new 'Viton' compound seals.
8/12/68	1113	Amplitude $\pm 10^\circ$ , frequency 0.5 cps. Conducted visual inspection. Detected relative motion between damper arm and shaft.  Cause: Improper torque on nut.  Corrective Action: Retorqued.
8/23/68	1181	Front seal oil seepage.  Cause: Initial failure of sealing lip.  Corrective Action: Replenished oil and continued operating, since no increase in temperature occurred.
8/26/68	1213	Amplitude $\pm 15^\circ$ , frequency 0.5 cps. Visual inspection conducted. System functioned satisfactorily.

<u>Date</u>	<u>Test Hour</u>	<u>Remarks</u>
8/27/68	1238	Amplitude $\pm 17^\circ$ , frequency 0.5 cps. Visual inspection conducted. System functioned satisfactorily.
8/28/68	1264	Amplitude $\pm 5^\circ$ , frequency 0.5 cps. Front and rear transmission seals leaking. Temperature increased to 200°F.  Cause: Breakdown of seal lips.  Corrective Action: Seals replaced. Oil replenished.
8/29/68	1281	Both transmission seals leaking. Temperature increased to 250°F.  Cause: Seal failure.  Corrective Action: Changed seal design and gear lubricant. Installed felt dust seals and lubricated gears with silicone grease, medium grade, Dow Corning No. 33.
9/10/68	1281	Resumed testing. Temperature stabilized at 100-110°F.
9/15/68	1376	Amplitude $\pm 10^\circ$ , frequency 0.5 cps. Conducted visual inspection. System functioned satisfactorily.
9/19/68	1480	Amplitude $\pm 15^\circ$ , frequency 0.5 cps. Table wave form altered from sinusoidal to nearly square. Corrective action not taken due to time limitation.
9/20/68	1500	Amplitude $\pm 5^\circ$ , frequency 1.0 cps. Visual inspection conducted. System operated satisfactorily.

<u>Date</u>	<u>Test</u> <u>Time</u>	<u>Remarks</u>
10/4/68	1735	Amplitude -30", frequency 1.8 cps. Visual inspection conducted. Some link imperfections. Corrective action not considered essential.
10/5/68	1752	System shut down. Excessive vibration. Radial and radial play noted in plant axle bearings.  Cause: Plant bearings not preloaded radially during assembly (see inspection report). Temporary corrective actions were taken to minimize vibration and to complete operational test, since fabrication of several new parts was required for a permanent fix.
10/13/68	1752	Tests were resumed.
10/23/68	1825	Vibration level increased due to continuous degradation of table wave drive input. Tests were terminated.

## 1. THE M&M INSPECTED MIPMC

The M&M consisting of the Dynaguns and the Heading Assist Gun was disassembled after completion of the evaluation tests, and the major components were inspected with the following results:

### 1. Dynaguns

**Bearing:** All bearings were checked for axial play and roughness. They were found to be in serviceable condition.

**Universal Joint:** There was no indication of increased angular clearance in the universal joint.

**Damper Rods:** The damper rod assemblies were weighed and the results compared with their original weights as shown in

Table VI. The wear rates (i.e., reduction of weight per unit time) shown in the table are considered to be negligible.

Damper Tracks: The modified design damper tracks were not hardened after approximately 500 hours of operation.

Drive Shaft: The multiplex discslide lubricated shaft showed no additional evidence of increased wear.

Drive Spline: Good condition.

TABLE VI							
WEIGHTED DAMPER TRACKS - GROSS WEIGHT							
		Track			Weights - Gross		Pod
Assembly	Track	1000	750	500	1000	750	500
1		14.1676	14.1782	14.1888	11.0345	11.0346	11.0348
2		13.1343	13.1356	13.1369	10.9985	10.9978	10.9980
3		13.0610	13.0620	13.0630	11.0649	11.0643	11.0650

The increase in weight reflected by the damper track is attributed to the transfer of lubricant from the Gilite track.

The net weight change occurred for assembly 1:

$$\begin{aligned}
 &\text{Track weight} - .0017 \\
 &\text{Rod weight} + .0015 \\
 &\text{Net reduction} .0002 \text{ gms}
 \end{aligned}$$

This results in a calculated wear rate of  $.0022 \times 10^{-3}$  in./inch of travel, which is considered to be negligible.

## **2. Heading Assist Gyro**

**Bearings:** Pivot bearings - no wear noted. Axial and radial motion of approximately 0.002 inch was measured on the output shaft adjacent to the upper bearing. Intermediate bearings exhibited no wear.

**Universal Joint:** There was no indication of increased angular clearance in the unit.

**Transmission Gear Assembly:** The transmission planetary gear train did not exhibit measurable wear. The gear train was lubricated with Dow Corning 33 medium grade grease.

**Drive Shaft:** The splined shaft driven by the hydraulic motor showed no signs of wear or corrosion.

**Pivot Bearing Housing:** Bore diameter increased 0.003 inch.

**Pivot Bushing:** Diameter was reduced by 0.0025 inch.

**Pivot Shaft:** Diameter was reduced by 0.001 inch.

Unclassified

Security Classification

DOCUMENT CONTROL DATA - R & D		
(Security classification of title, body of abstract and indexing annotation must be entered when the overall report is classified)		
1. ORIGINATING ACTIVITY (Corporate author)		2a. REPORT SECURITY CLASSIFICATION
Dynasciences Corporation Blue Bell, Pennsylvania		Unclassified
		2b. GROUP
3. REPORT TITLE		
RELIABILITY EVALUATION OF A MECHANICAL STABILITY AUGMENTATION SYSTEM FOR HELICOPTERS		
4. DESCRIPTIVE NOTES (Type of report and inclusive dates)		
Final Report - DCR-284 March 1967 to December 1968		
5. AUTHOR(S) (First name, middle initial, last name)		
Mario M. George Edmund M. Fraundorf Eugene Kisielowski		
6. REPORT DATE	7a. TOTAL NO. OF PAGES	7b. NO. OF REFS
June 1969	93	2
8a. CONTRACT OR GRANT NO.	8b. ORIGINATOR'S REPORT NUMBER(S)	
DAAJ02-67-G-0029	USAAVLABS Technical Report 69-17	
9. PROJECT NO.	9b. OTHER REPORT NO(S) (Any other numbers that may be assigned this report)	
Task 1F162204A13905	DCR-284	
10. DISTRIBUTION STATEMENT		
<del>This document has been approved for public release and unlimited distribution.</del>		
11. SUPPLEMENTARY NOTES		12. SPONSORING MILITARY ACTIVITY
		U.S. Army Aviation Materiel Laboratory, Ft. Eustis, Virginia
13. ABSTRACT		
<p>This report presents the results of a reliability evaluation of a flightworthy, compact, lightweight three-axis mechanical stability augmentation system (MSAS) for helicopters. The MSAS consists of the Dynagyro, a two-axis coulomb damped gyroscope, and the Heading Assist Gyro, a single-axis spring-damped rate gyroscope. As part of this program, a prototype flightworthy model of the MSAS was designed, fabricated and extensively tested to evaluate the reliability and maintainability of the system. The results of these tests have demonstrated that the MSAS has excellent stability augmentation characteristics, is mechanically reliable, and is easy to maintain.</p>		

DD FORM 1473

REPLACES DD FORM 1473, 1 JAN 64, WHICH IS OBSOLETE FOR ARMY USE.

Unclassified

Security Classification



Unclassified

Security Classification

14. KEY WORDS	LINK A		LINK E		LINK C	
	ROLE	WT	ROLE	WT	ROLE	WT
Stability Control Gyroscope Mechanical Mechanical Stability Augmentation System Reliability						

Unclassified

Security Classification

1675-69